Supplementary Information:

Dimensional Control of Low-Dimensional Perovskite Hybrids for Photovoltaics

Fei Wang[1†], Xiang Zhang[2†], Jinfeng Zeng[3†], Xi Wang[4,5†], Xueping Liu[6], Kang Zhou[1], Hao Wang[1], Chunming Yang[7], Haoran Lin[1], Yumeng Shi[8], Wenzhu Liu[9], Yonghua Chen[10], Mingjian Yuan[11], Jingbai Li[1]*, Hu Chen[3]*, Wei Zhang[6,12]*, Yi Hou[4,5]*, Hao Chen[2]*, Hanlin Hu[1]*

[1]Hoffmann Institute of Advanced Materials, Shenzhen Polytechnic University, 7098 Liuxian Boulevard, Shenzhen 518055, China

[2]Center of Future Photovoltaics Research, Global Institute of Future Technology (GIFT), Shanghai Jiao Tong University, Shanghai, 200240, China

[3]School of Physical Sciences, Great Bay University, Dongguan, 523000, China; Great Bay Institute for Advanced Study, Dongguan, 523000, China

[4]Department of Chemical and Biomolecular Engineering, National University of Singapore, Singapore, Singapore

[5]Solar Energy Research Institute of Singapore (SERIS), National University of Singapore, Singapore, Singapore

[6]Advanced Technology Institute, University of Surrey, Guildford GU2 7XH, United Kingdom

[7]Shanghai Synchrotron Radiation Facility, Shanghai Advanced Research Institute, Chinese Academy of Sciences, Shanghai, 201204, China

[8]Key Laboratory of Luminescence and Optical Information, Ministry of Education, Institute of Optoelectronic Technology, Beijing Jiaotong University, Beijing, 100044, China

[9]Research Center for New Energy Technology, Shanghai Institute of Microsystem and Information Technology, Chinese Academy of Sciences, Shanghai, 200050, China

[10]Key Laboratory of Flexible Electronics (KLoFE) & Institute of Advanced Materials (IAM), School of Flexible Electronics (Future Technologies), Nanjing Tech University (NanjingTech), Nanjing, 211816, China

[11]College of Chemistry, Nankai University, Tianjin, 300071, China

[12]School of Materials Science and Engineering, Zhengzhou University, Zhengzhou, Henan Province, 450001, China.

[†]These authors contributed equally.

*Corresponding Authors. E-Mail address: lijingbai@szpu.edu.cn

chenhu@gbu.edu.cn

wz0003@surrey.ac.uk

yi.hou@nus.edu.sg

hao.chen1@sjtu.edu.cn

hanlinhu@szpu.edu.cn

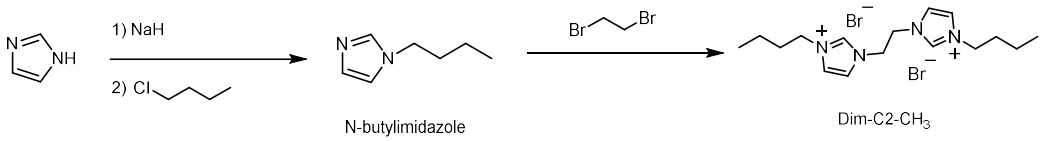

Supplementary Fig. 1 Synthetic route of Dim-C2-CH_3 molecule.

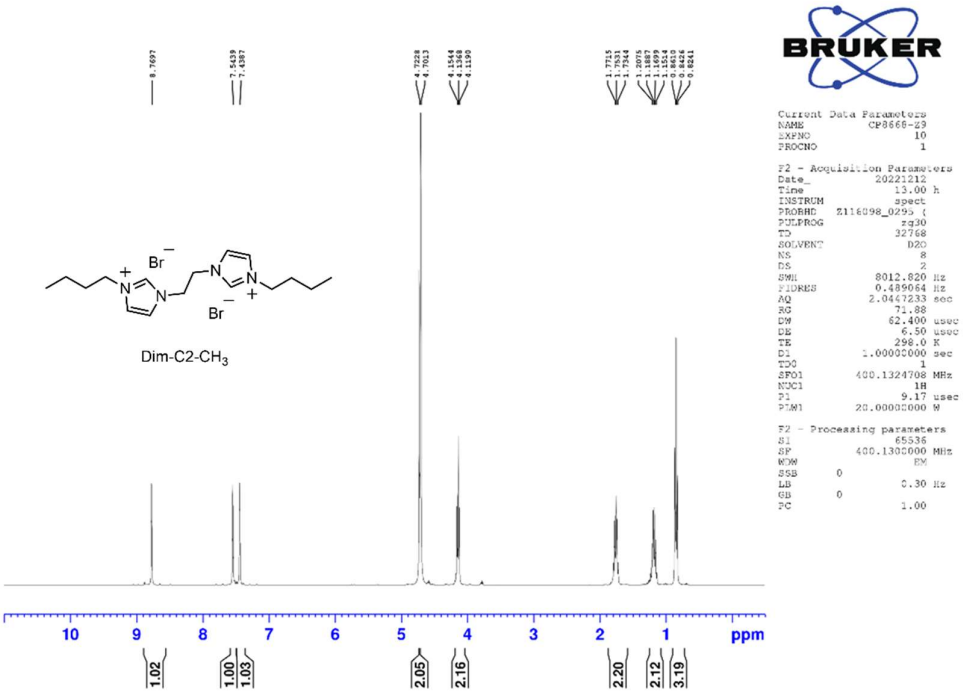

Supplementary Fig. 2 ^{1}H NMR spectrum of Dim-C2-CH_3 molecule.

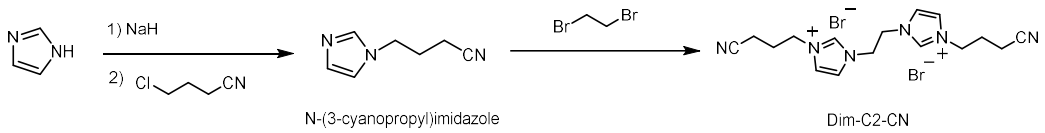

Supplementary Fig. 3 Synthetic route of Dim-C2-CN molecule.

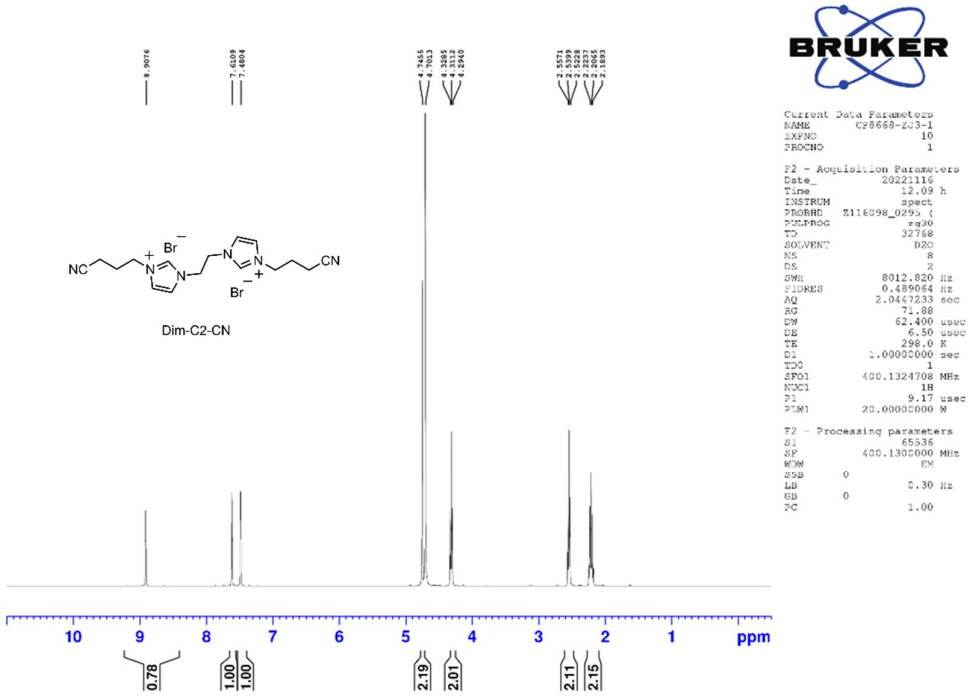

Supplementary Fig. 4 ^{1}H NMR spectrum of Dim-C2-CN molecule.

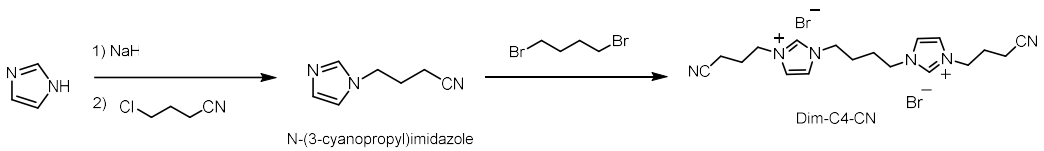

Supplementary Fig. 5 Synthetic route of Dim-C4-CN molecule.

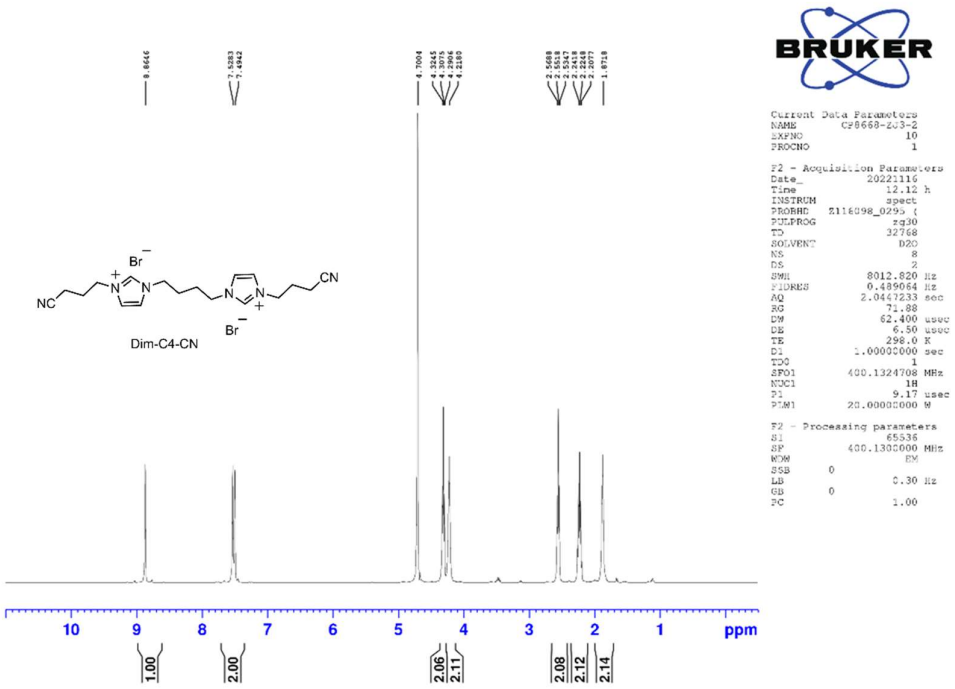

Supplementary Fig. 6 ^{1}H NMR spectrum of Dim-C4-CN molecule.

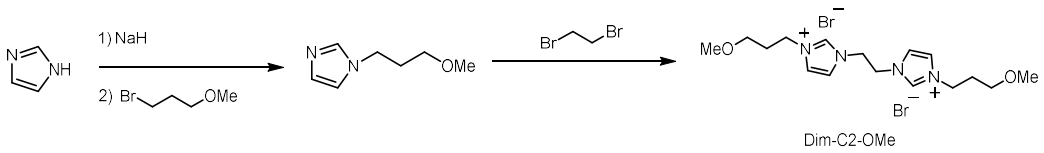

Supplementary Fig. 7 Synthetic route of Dim-C2-OMe molecule.

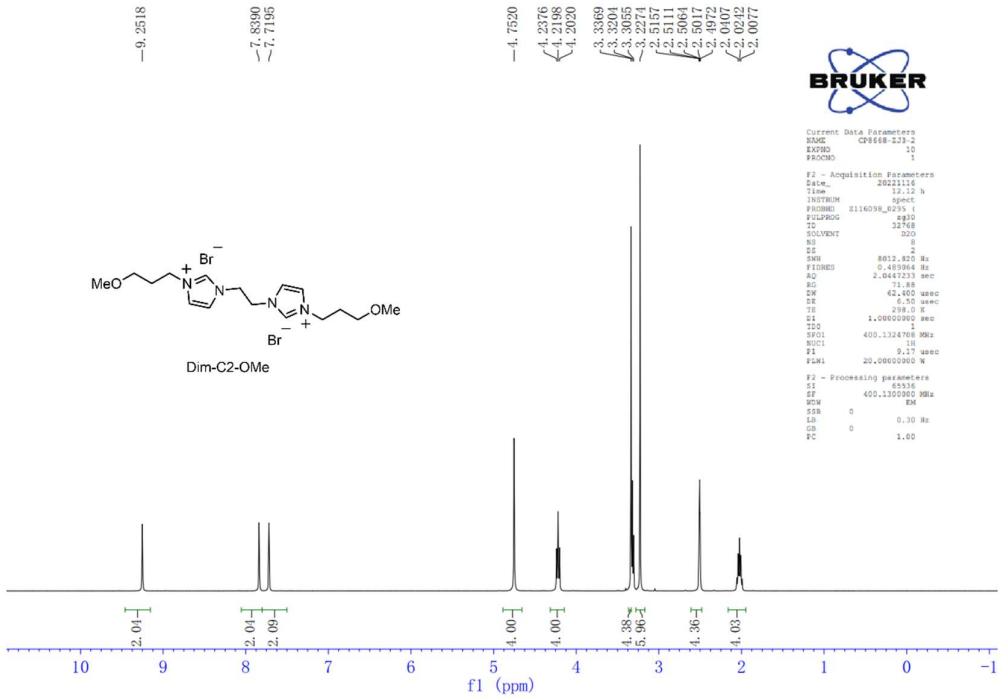

Supplementary Fig. 8 ^{1}H NMR spectrum of Dim-C2-OMe molecule.

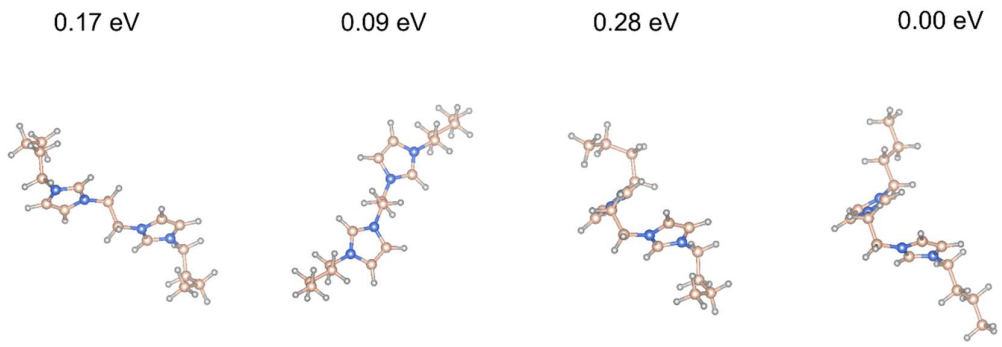

Supplementary Fig. 9 Optimized molecular configurations of Dim-C2-CH_3 in DMSO with the relative energies, computed at the PBE0/cc-pVTZ level.

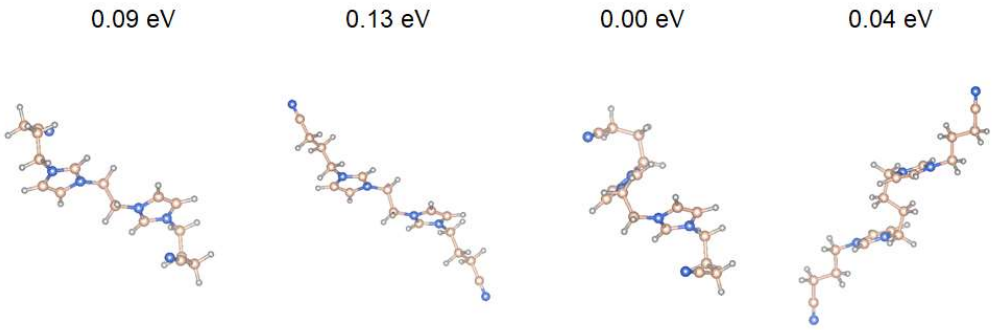

Supplementary Fig. 10 Optimized molecular configurations of Dim-C2-CN in DMSO with the relative energies, computed at the PBE0/cc-pVTZ level.

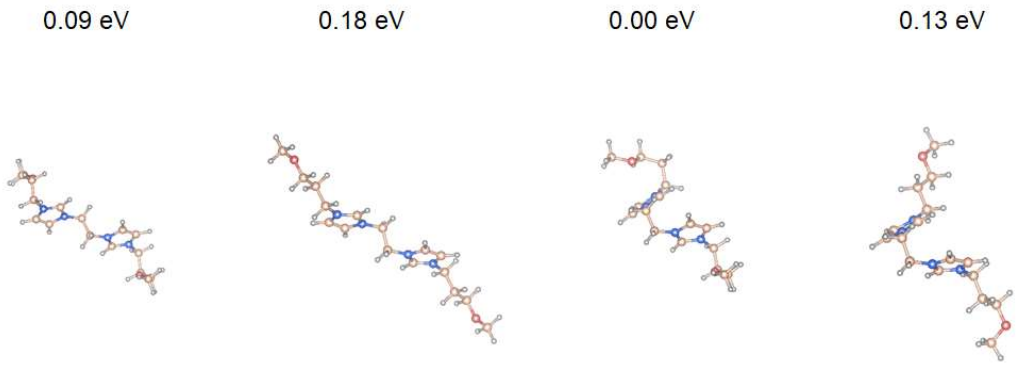

Supplementary Fig. 11 Optimized molecular configurations of Dim-C2-OMe in DMSO with the relative energies, computed at the PBE0/cc-pVTZ level.

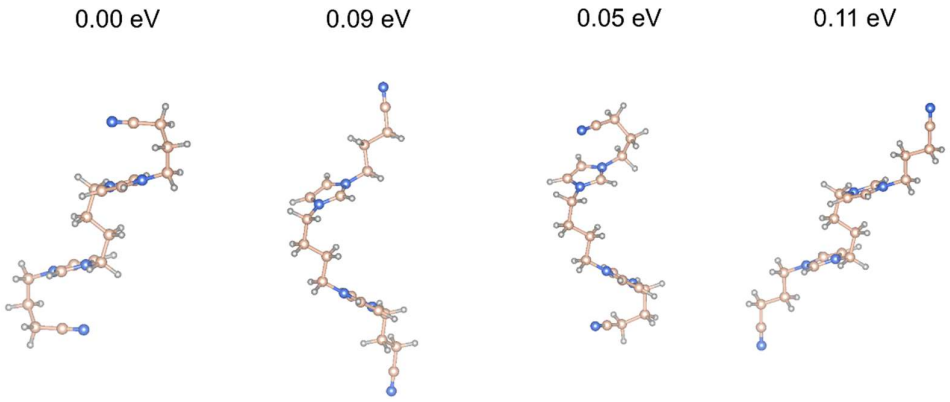

Supplementary Fig. 12 Optimized molecular configurations of Dim-C4-CN in DMSO with the relative energies, computed at the PBE0/cc-pVTZ level.

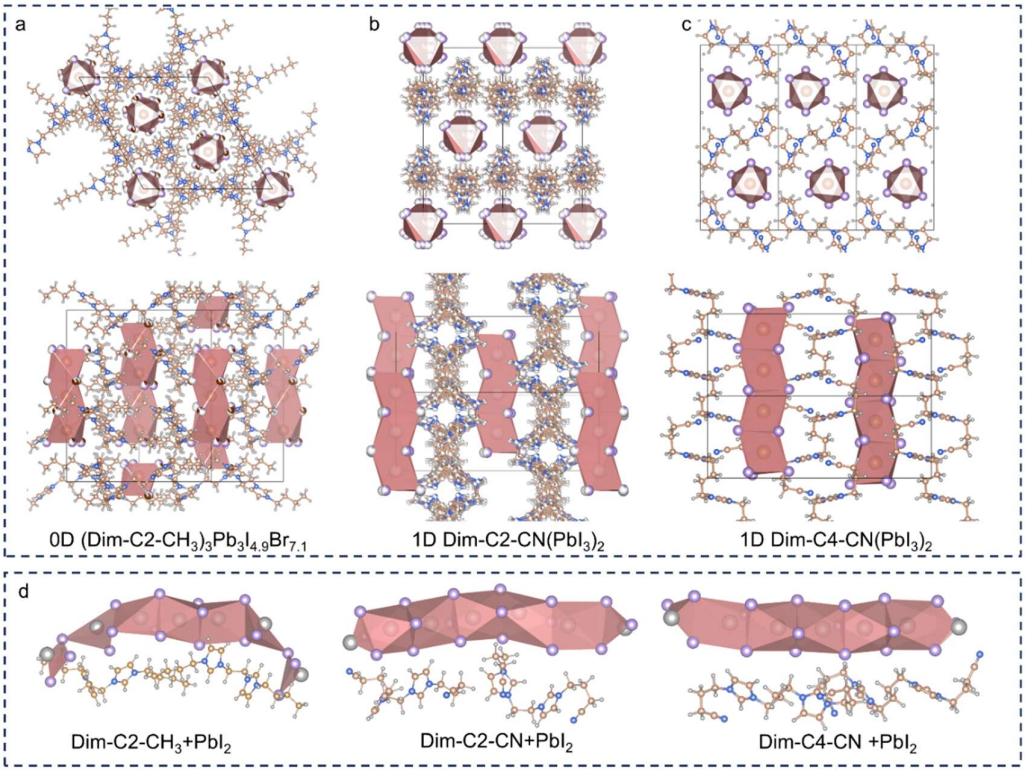

Supplementary Fig. 13 Single crystal structure analysis. The structural arrangements of (a) 0D $(Dim\text{-}C2\text{-}CH_3)_3Pb_3I_{4.9}Br_{7.1}$, (b) 1D $Dim\text{-}C2\text{-}CN(PbI_3)_2$ and (c) 1D $Dim\text{-}C4\text{-}CN(PbI_3)_2$ perovskites along different directions. Due to the disordered structure of the single crystal 1D $Dim\text{-}C2\text{-}CN(PbI_3)_2$, the optimized configuration after structural refinement is presented in Fig. 1c for analysis. (d) Molecular configurations of the ligands binding with a 1D PbI_2 cluster, optimized with DFT calculations.

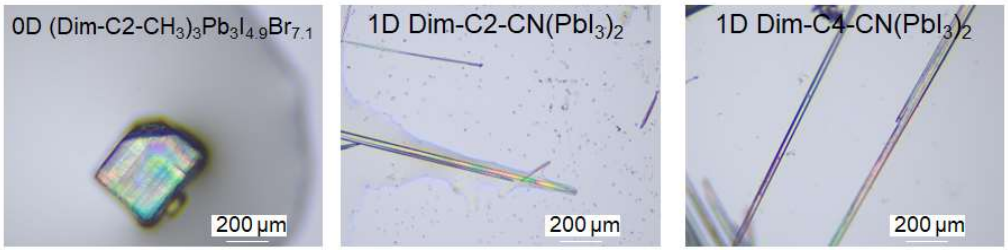

Supplementary Fig. 14 Optical micrograph of the 0D (Dim-C2-CH_3)$_3$$Pb_3I_{4.9}Br_{7.1}$, 1D Dim-C2-CN($PbI_3$)$_2$ and 1D Dim-C4-CN(PbI_3)$_2$ single crystals.

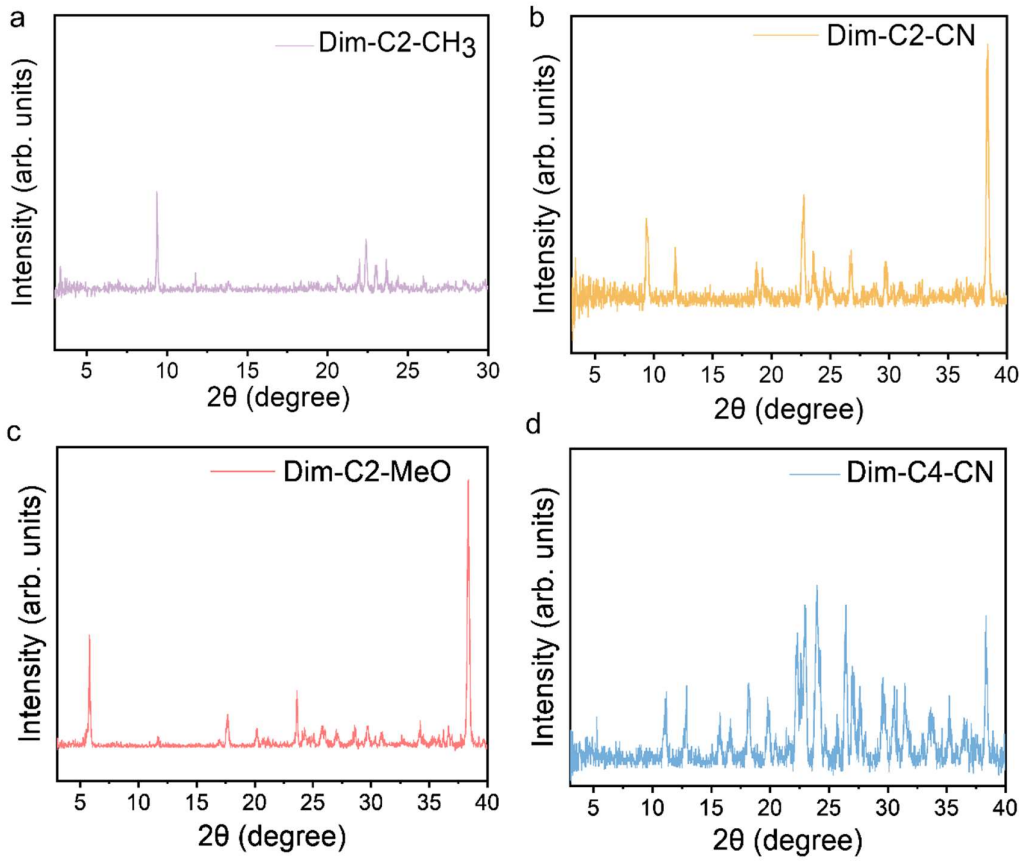

Supplementary Fig. 15 XRD patterns of organic ligands: Dim-C2-CH_3, Dim-C2-CN, Dim-C2-MeO and Dim-C4-CN.

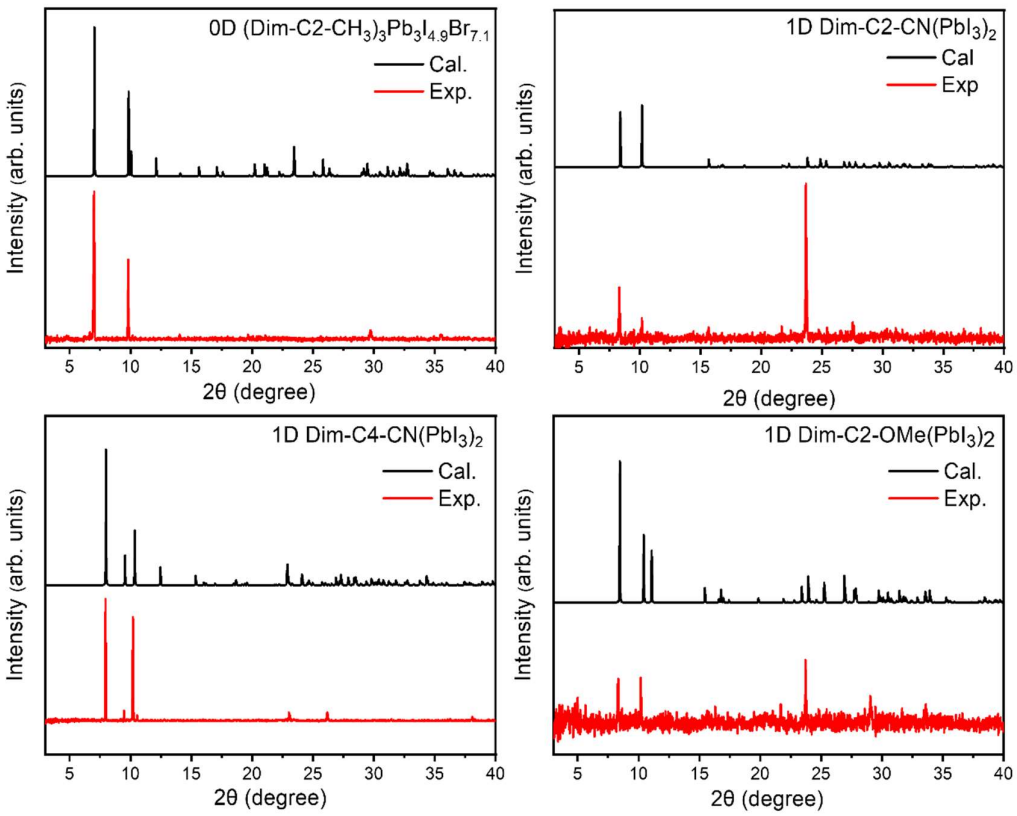

Supplementary Fig. 16 Powder and calculated XRD patterns of the (Dim-C2-CH_3)$_3$$Pb_3I_{4.9}Br_{7.1}$, Dim-C2-CN($PbI_3$)$_2$, Dim-C4-CN($PbI_3$)$_2$ and Dim-C2-OMe(PbI_3)$_2$ single crystals.

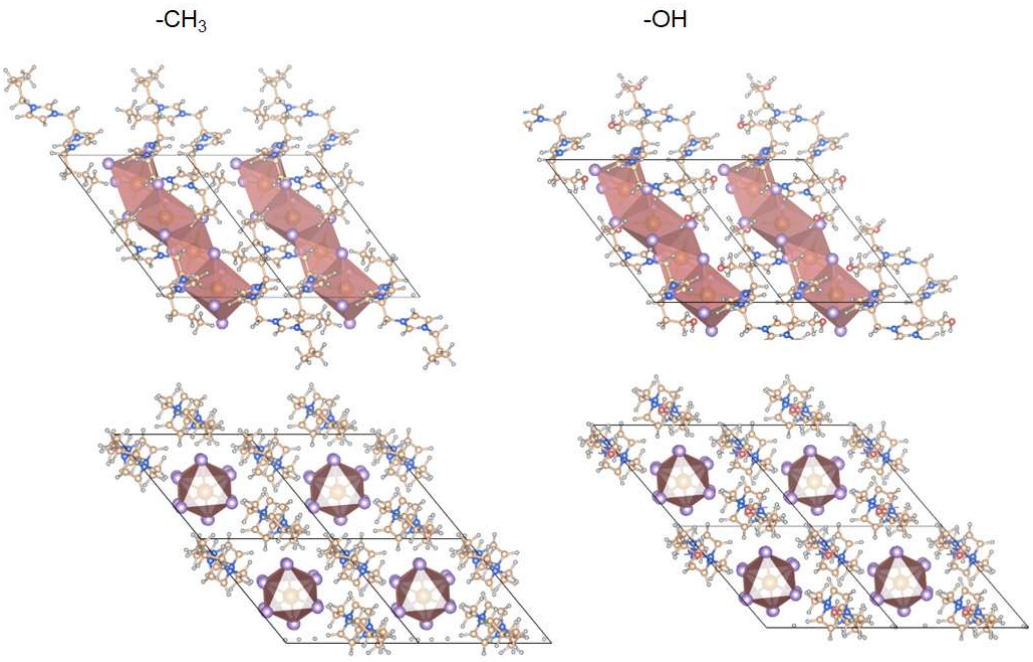

Supplementary Fig. 17 Side (first row) and top view (second row) of the DFT optimized crystal structures of Dim-C2-$CH_3(PbI_3)_2$ and Dim-C2-$OH(PbI_3)_2$.

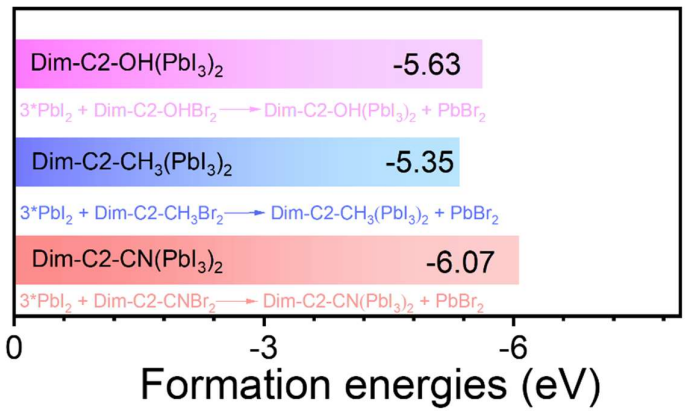

Supplementary Fig. 18 Formation energies of the Dim-C2-$CH_3(PbI_3)_2$, Dim-C2-$CH_3(PbI_3)_2$, and Dim-C2-$CH_3(PbI_3)_2$ crystals computed by DFT calculations.

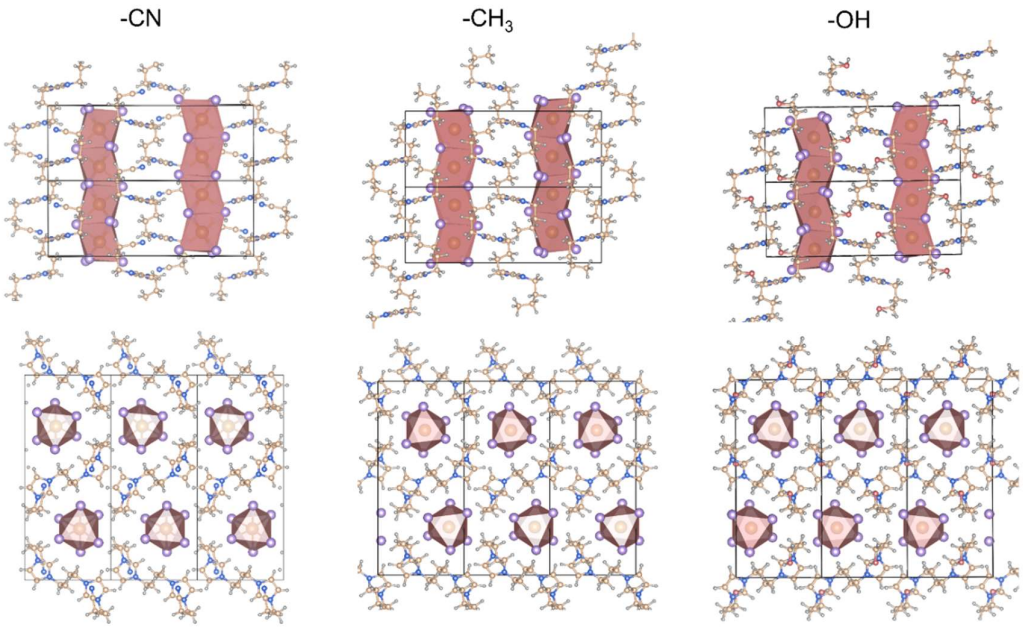

Supplementary Fig. 19 Crystal structure simulation. Simulation of the single crystal structure 1D Dim-C4-CN$(PbI_3)_2$ after replacing the -CN in the ligand Dim-C4-CN with a -CH_3 or -OH group.

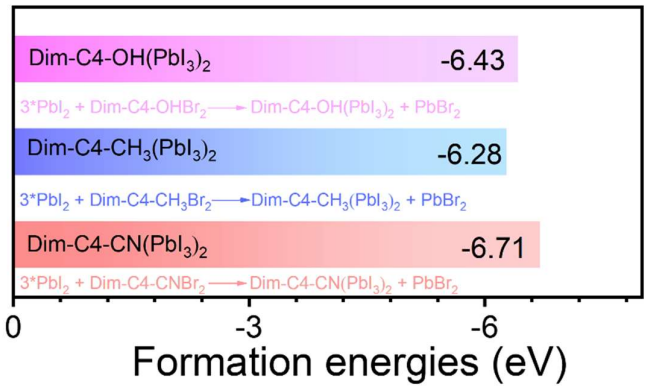

Supplementary Fig. 20 Formation energies of the Dim-C4-$CH_3(PbI_3)_2$, (Dim-C4-$CH_3(PbI_3)_2$, and Dim-C4-$CH_3(PbI_3)_2$ crystals computed by DFT calculations.

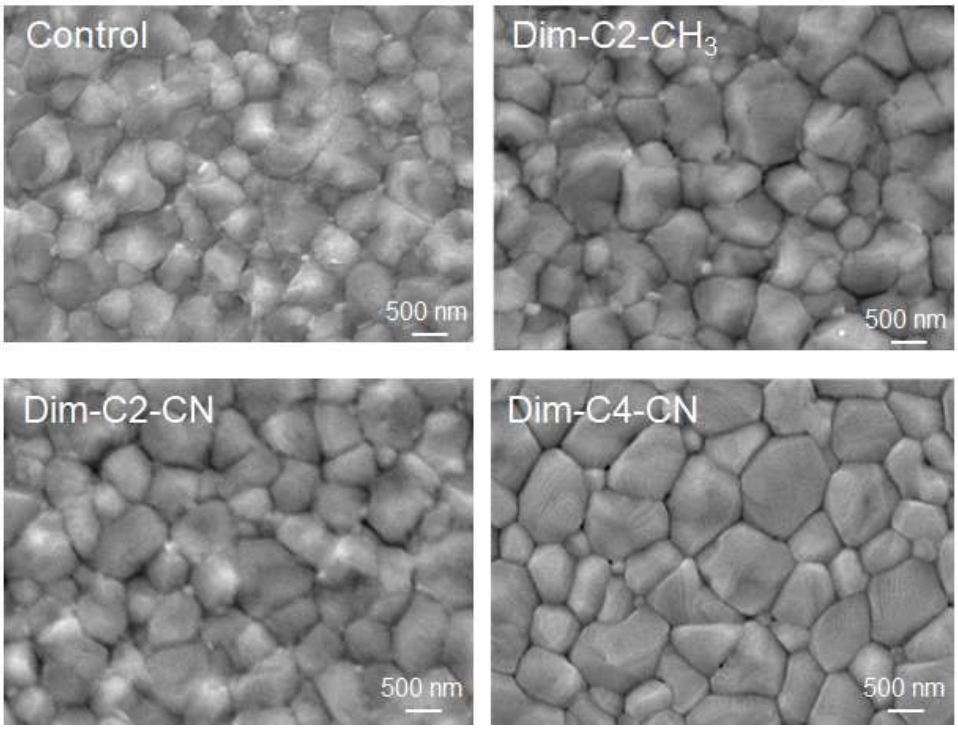

Supplementary Fig. 21 Top-view SEM characterization of the reference, Dim-C2-CH_3-, Dim-C2-CN-, and Dim-C4-CN-modified perovskite films.

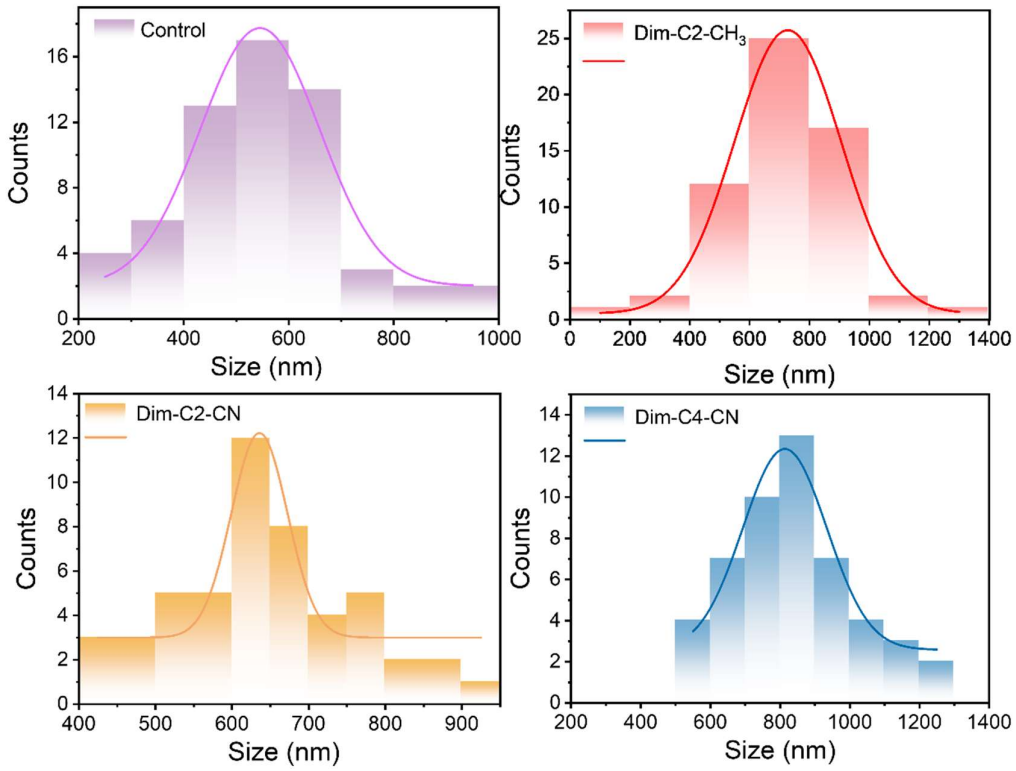

Supplementary Fig. 22 The grain size distribution of the reference, Dim-C2-CH_3-, Dim-C2-CN-, and Dim-C4-CN-modified perovskite film based on SEM image analysis. The average grain sizes of the four films were measured to be 545 nm (reference), 727 nm (Dim-C2-CH_3- modified perovskite film), 635 nm (Dim-C2-CN-modified perovskite film), and 813 nm (Dim-C4-CN-modified perovskite film), respectively.

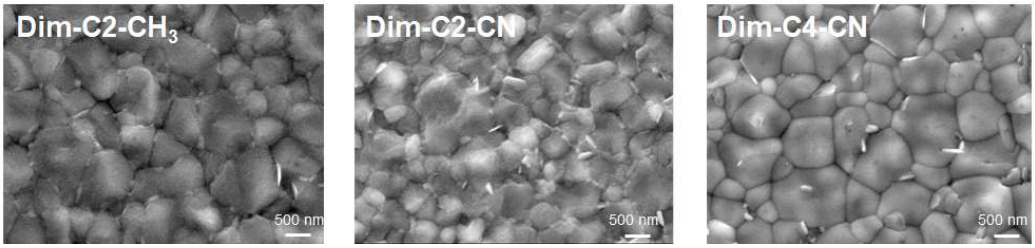

Supplementary Fig. 23 Top-view SEM images of perovskite films treated with high-concentration ligands (0.5 mg/mL).

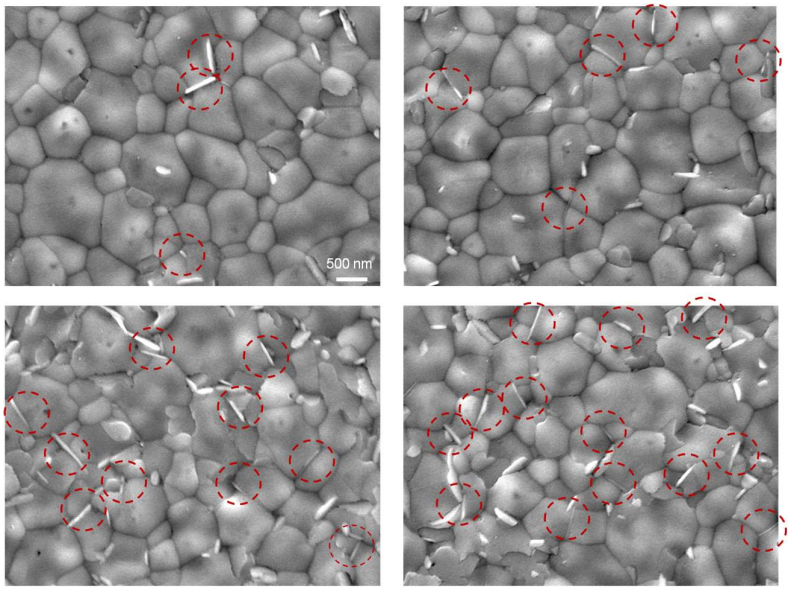

Supplementary Fig. 24 Top-view SEM images of perovskite films treated with Dim-C4-CN at concentrations of 0.3, 0.5, 0.75, and 1.0 mg/mL.

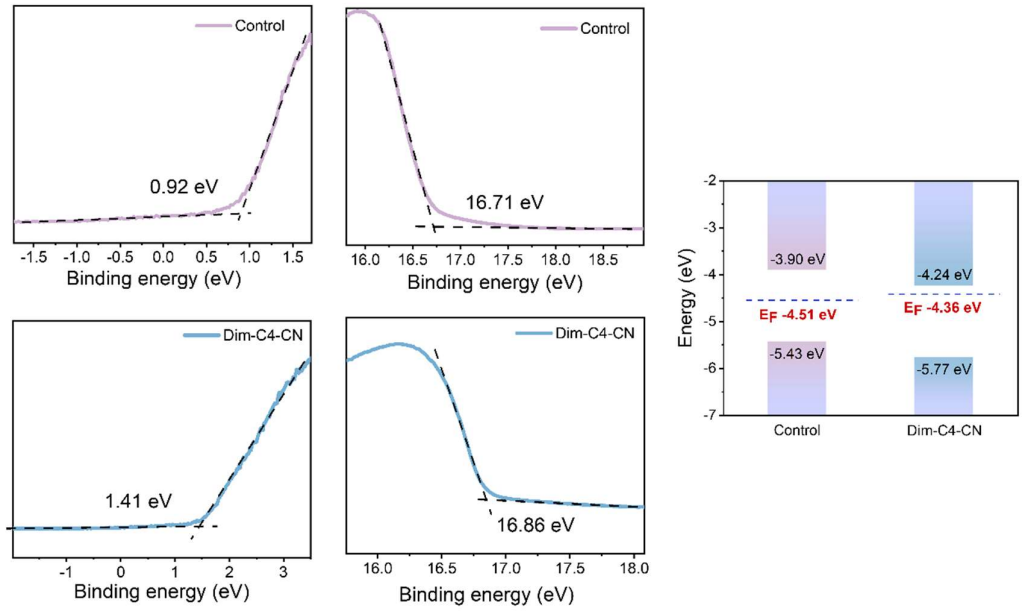

Supplementary Fig. 25 UPS spectra for Fermi edge ($E_{F,\ edge}$) and cut-off energy ($E_{cut\text{-}off}$) of control and Dim-C4-CN-modified perovskite samples. The Fermi level (E_F) values were calculated as −4.51 and −4.36 eV using the formula $E_F = E_{cut\text{-}off} - 21.22$. The Fermi edges ($E_{F,edge}$) for control perovskite and Dim-C4-CN-modified perovskite films were estimated at 0.92 and 1.41 eV, respectively. Furthermore, the valance band maximum (VBM) of the control and Dim-C4-CN-modified perovskite films were computed as −5.43 and −5.77 eV, respectively.

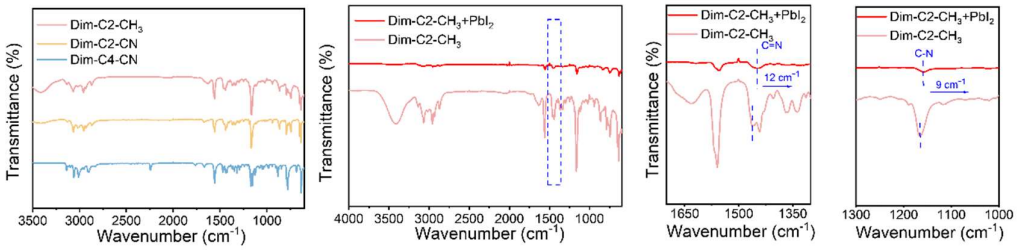

Supplementary Fig. 26 FTIR spectra of Dim-C2-CH_3, Dim-C2-CN, Dim-C4-CN and Dim-C2-CH_3+PbI_2 samples.

The interactions between three ligands and perovskite components were thoroughly investigated using FTIR and NMR spectra. FTIR spectra of the ligand+PbI_2 samples revealed strong interactions between the imidazole rings of all three ligands and PbI_2, which was further confirmed by NMR analysis. Additionally, the cyano groups in Dim-C2-CN and Dim-C4-CN also exhibited strong interactions with PbI_2. When these ligands were added to the PbI_2 precursor solution and corresponding films were prepared, the lightened color of the resulting PbI_2 films further confirmed the strong ligand-z_2 interactions.

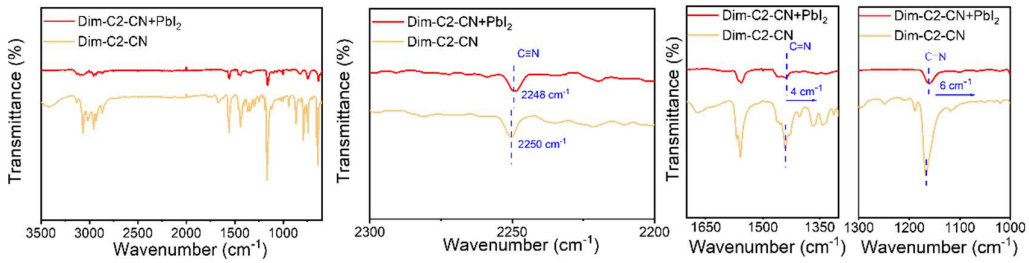

Supplementary Fig. 27 FTIR spectra of Dim-C2-CN and Dim-C2-CN+PbI_2 samples.

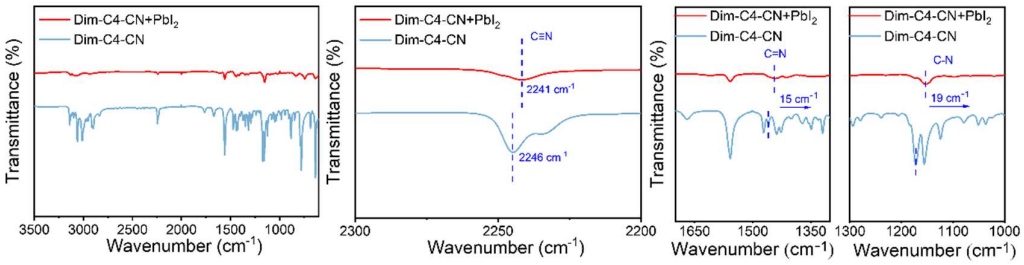

Supplementary Fig. 28 FTIR spectra of Dim-C4-CN and Dim-C4-CN+PbI_2 samples.

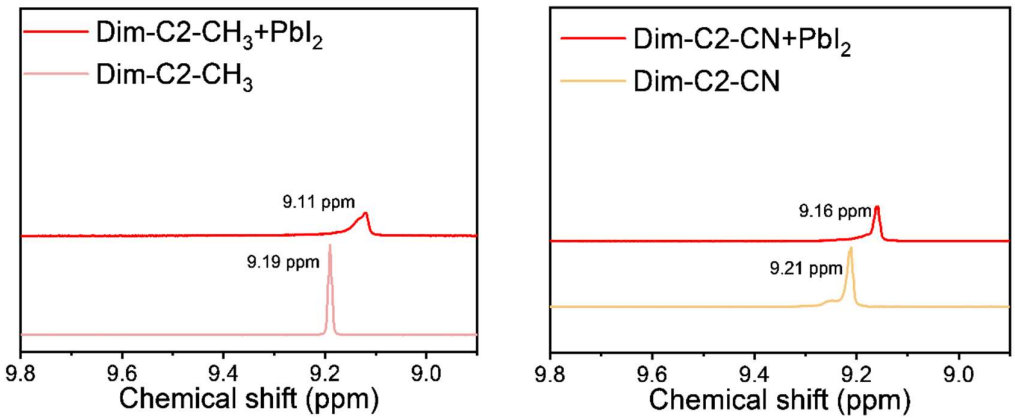

Supplementary Fig. 29 NMR spectra of Dim-C2-CH_3/Dim-C2-CN, Dim-C2-CH_3/Dim-C2-CN+PbI_2 samples.

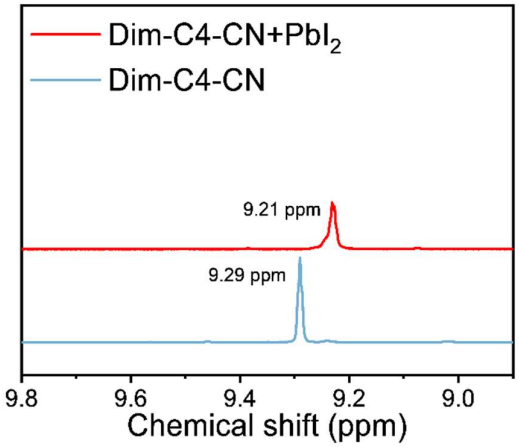

Supplementary Fig. 30 NMR spectra of Dim-C4-CN and Dim-C4-CN+PbI_2 samples.

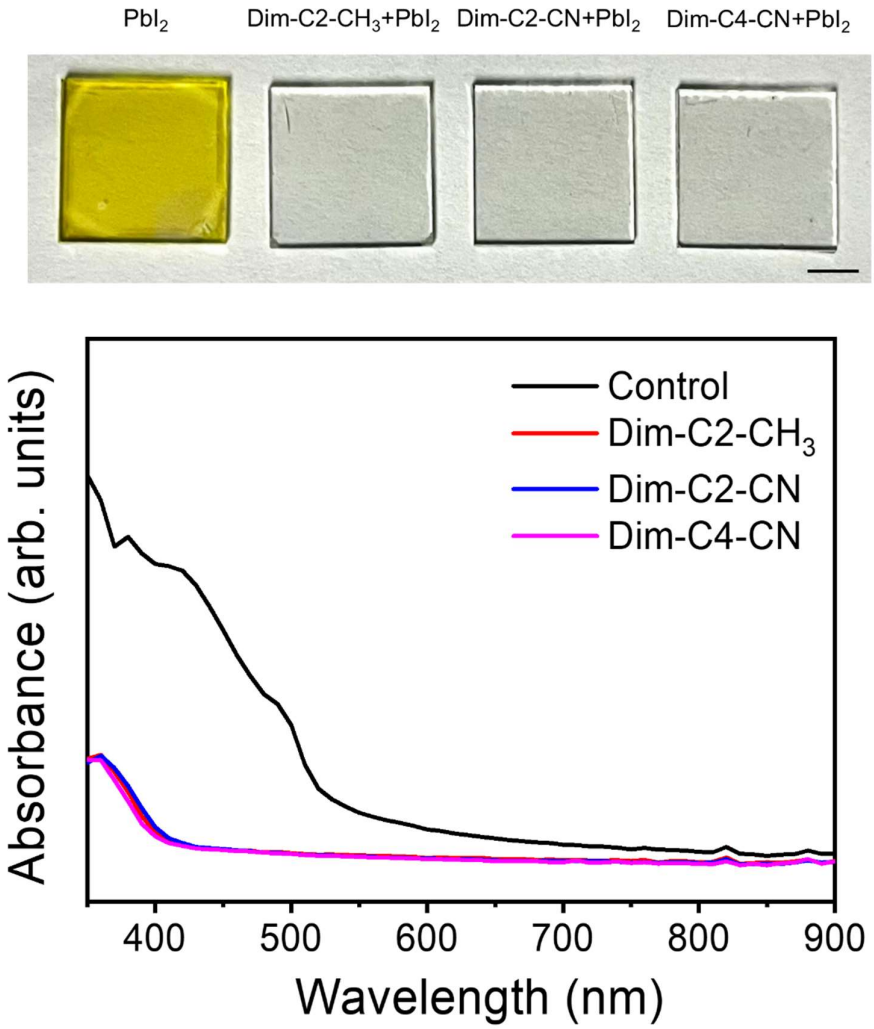

Supplementary Fig. 31 Ligand-modified PbI_2 films and their corresponding UV-Vis absorption spectra. Sacle bar: 500 mm. The sample dimensions are 2 cm (length) × 2 cm (width).

When these ligands were added to the PbI_2 precursor solution and corresponding films were prepared, the lightened color of the resulting PbI_2 films further confirmed the strong ligand-PbI_2 interactions.

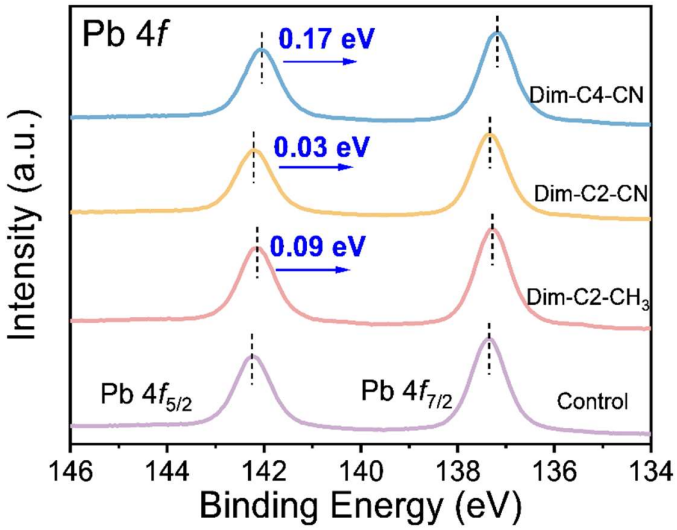

Supplementary Fig. 32 XPS spectra of reference, Dim-C2-CH_3-, Dim-C2-CN-, and Dim-C4-CN-modified perovskite films.

These robust interactions between the three ligands and PbI_2 provide the foundation for forming low-dimensional perovskites and passivating defects. X-ray photoelectron spectroscopy (XPS) analysis was systematically performed to probe the surface chemical states of lead species in the perovskite films (Fig. S32). The high-resolution Pb 4*f* spectra revealed consistent downward shifts in binding energies for both the Pb 4*f* 7/2 and Pb 4*f* 5/2 orbitals across all modified films. Notably, the Dim-C4-CN-treated sample demonstrated the most significant chemical shift (0.17 eV), which was attributed to enhanced electron density redistribution resulting from strong interactions between the Dim-C4-CN ligand and PbI_3^- octahedra.

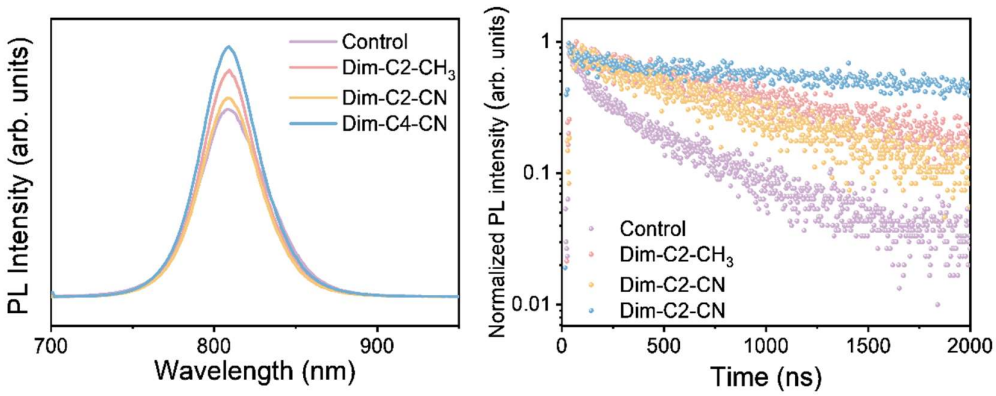

Supplementary Fig. 33 Steady-state PL and TRPL spectra of reference, Dim-C2-CH_3-, Dim-C2-CN-, and Dim-C4-CN-modified perovskite films.

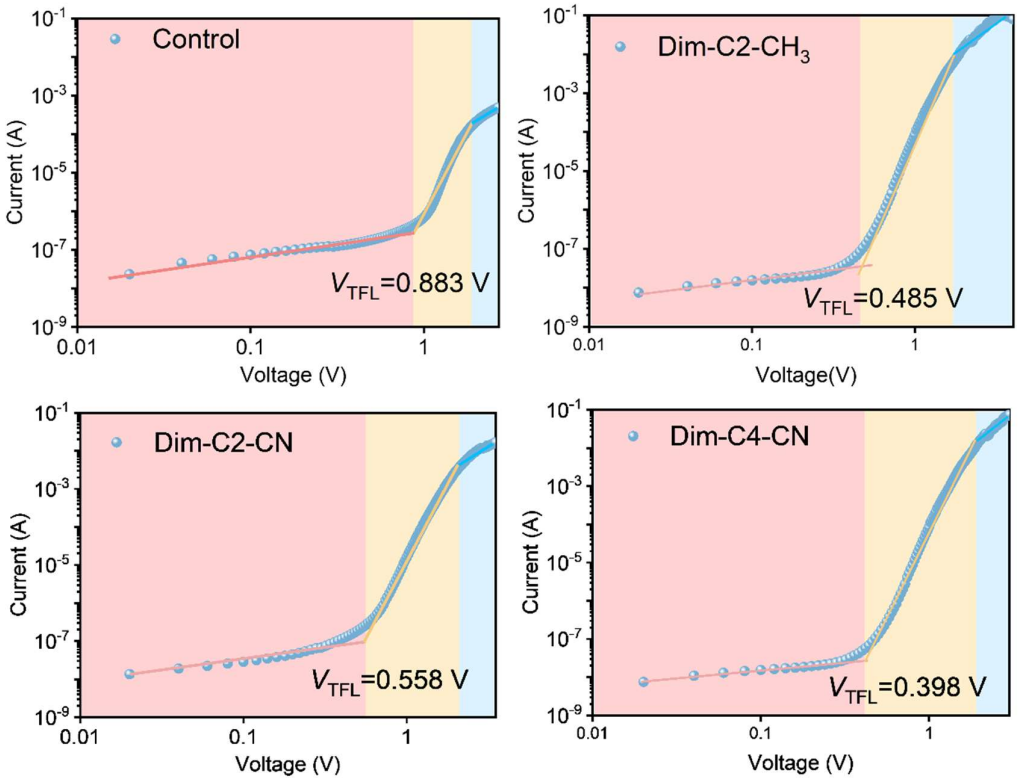

Supplementary Fig. 34 SCLC tests of reference, Dim-C2-CH_3-, Dim-C2-CN-, and Dim-C4-CN-modified perovskite devices.

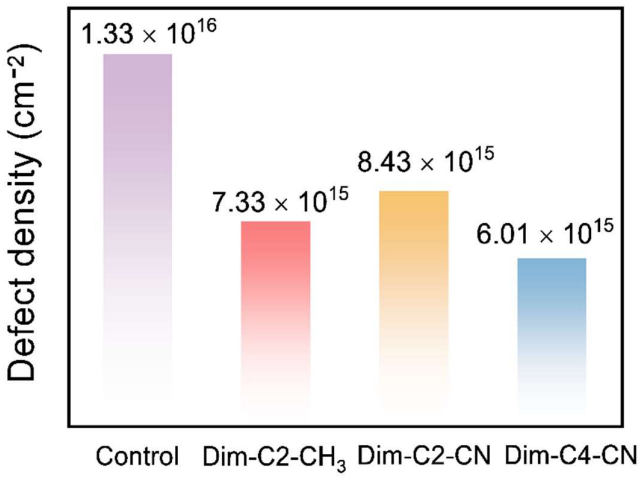

Supplementary Fig. 35 Statistics of defect density calculated from SCLC tests.

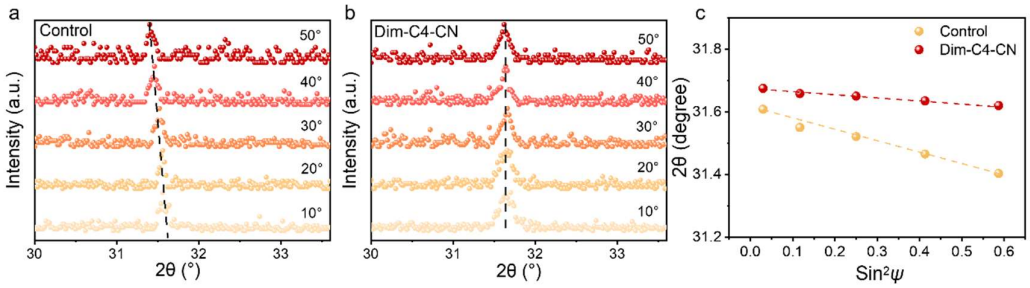

Supplementary Fig. 36 GIXRD patterns for both the (a) control and (b) Dim-C4-CN-modified perovskite films utilizing various instrumental ψ values ranging from 10 to 50°. (c) The linear fitting of 2θ-Sin$^2\psi$ for both control and Dim-C4-CN-modified perovskite films.

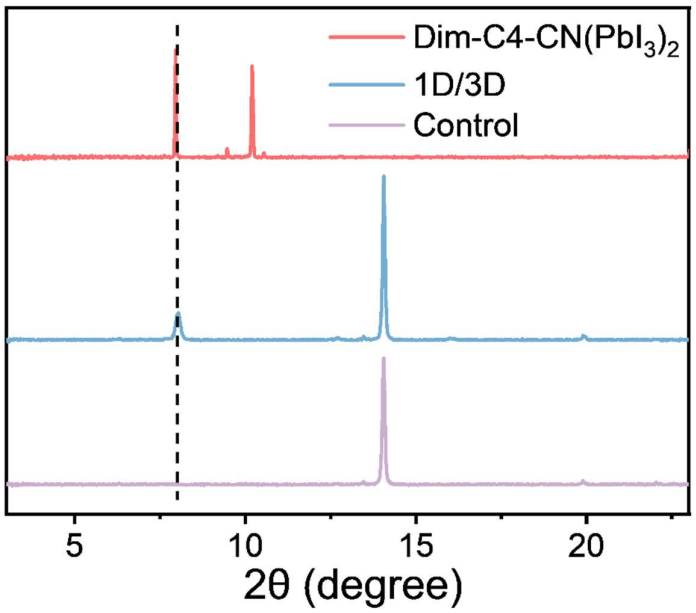

Supplementary Fig. 37 XRD patterns of single crystal Dim-C4-CN(PbI_3)$_2$, reference perovskite film and Dim-C4-CN-modified perovskite film.

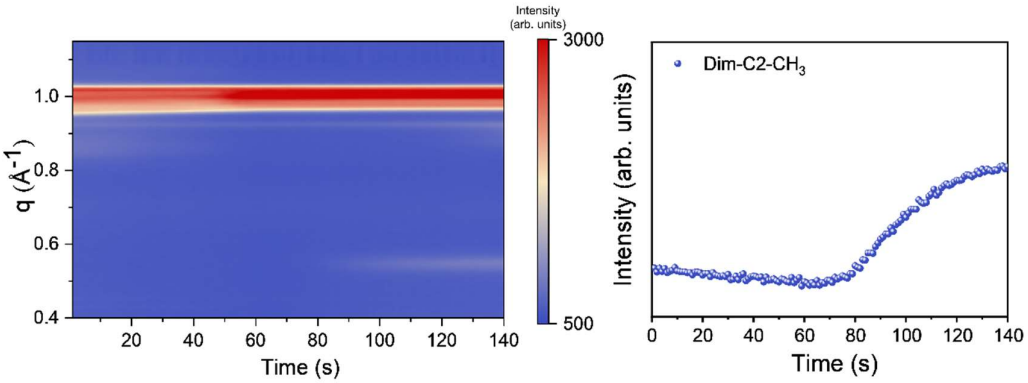

Supplementary Fig. 38 Time-resolved GIWAXS patterns during annealing of Dim-C2-CH_3-modified perovskite films.

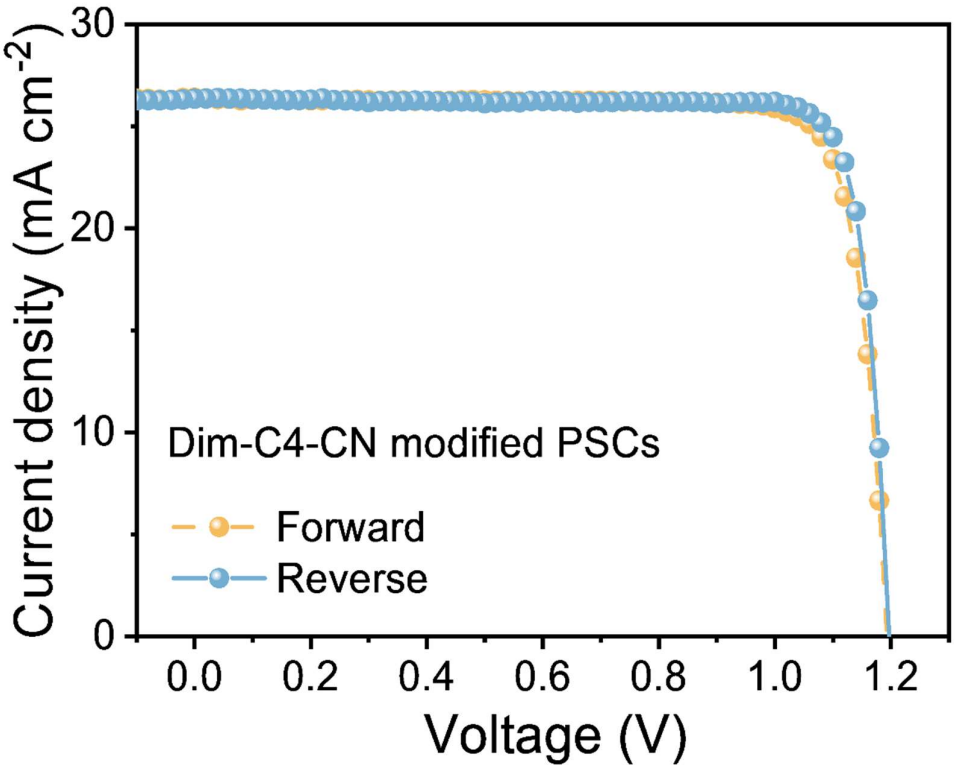

Supplementary Fig. 39 *J-V* curves under forward and reverse scans for the champion device.

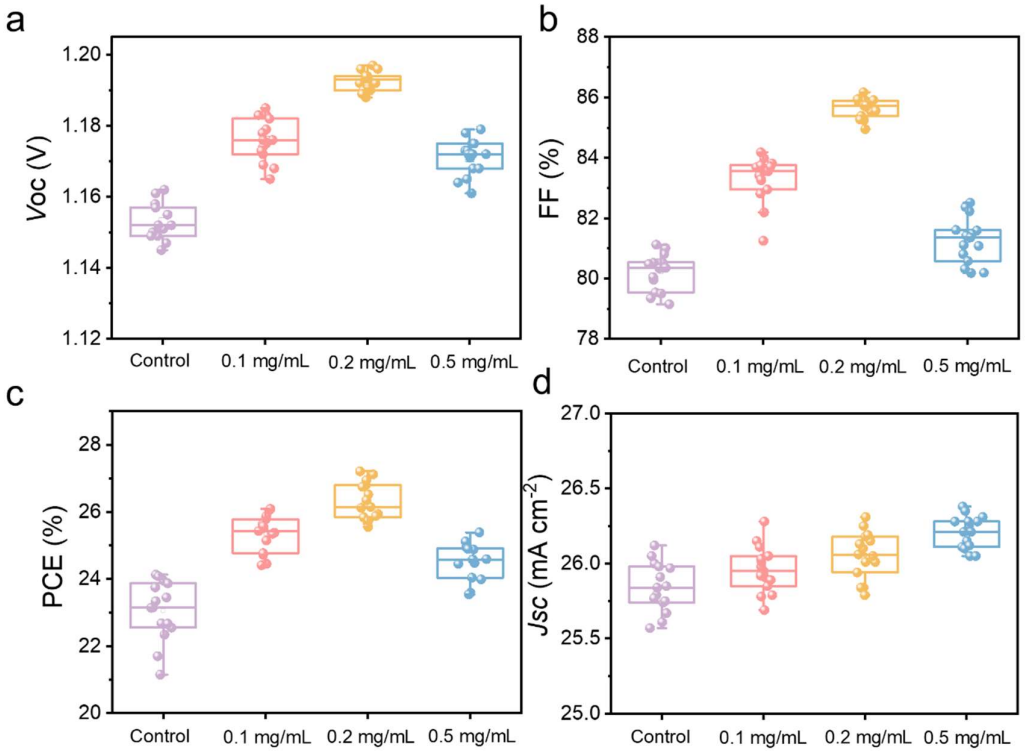

Supplementary Fig. 40 Photovoltaic performance statistics of the devices treated with varying concentrations of Dim-C4-CN. The statistics of photovoltaic performance parameters of control and ligands-modified PSCs: (a) V_{OC}, (b) FF, (c) PCE and (d) J_{SC}. In the box plots, the central line denotes the median, the square indicates the mean, the box bounds represent the 25th and 75th percentiles, while the whiskers extend to the furthest data points within 1.5 times the interquartile range.

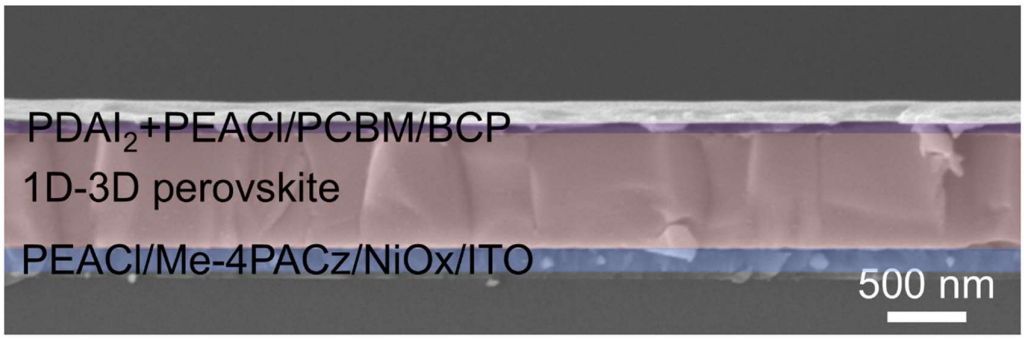

Supplementary Fig. 41 Cross-sectional SEM images of the Dim-C4-CN-modificated device. The device adopts a conventional inverted structure with the specific architecture of ITO/NiO_x/Me-4PACz/1D-3D perovskite/$PDAI_2$+PEACl/PCBM/BCP/Ag.

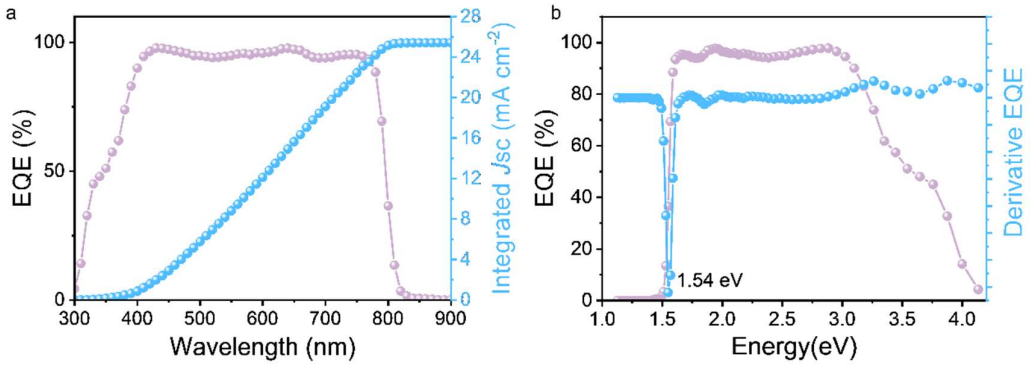

Supplementary Fig. 42 (a) EQE spectrum of the Dim-C4-CN modified device. (b) The bandgap energy calculated from the EQE spectrum is 1.54 eV.

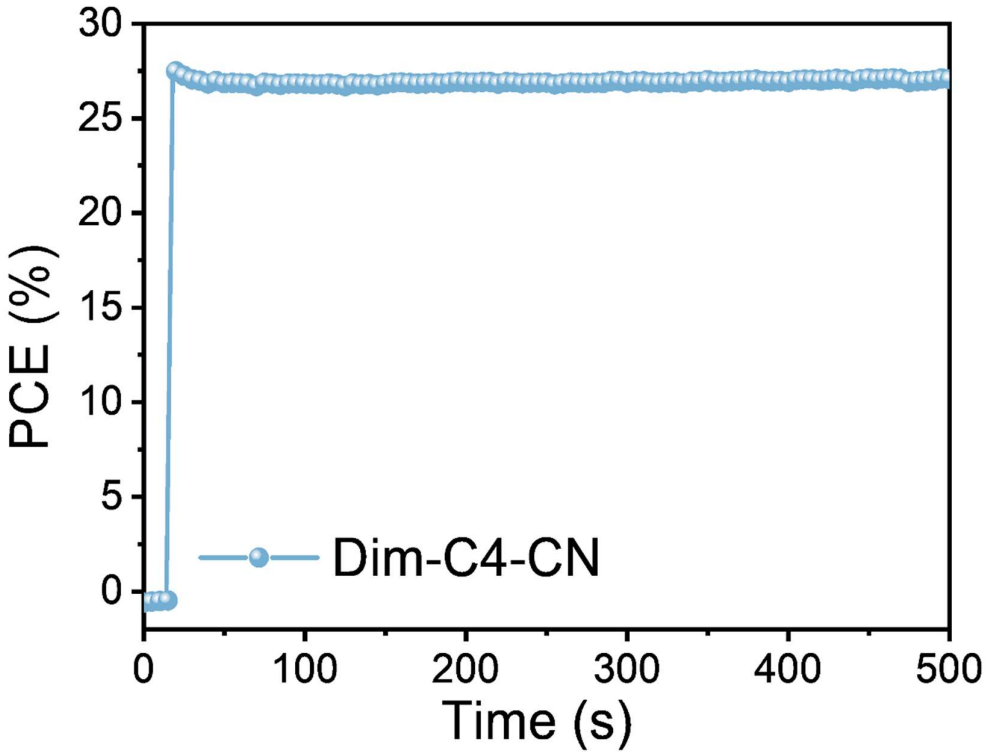

Supplementary Fig. 43 Steady-state PCE of Dim-C4-CN-modified under continuous AM 1.5G illumination at maximum power point tracking condition.

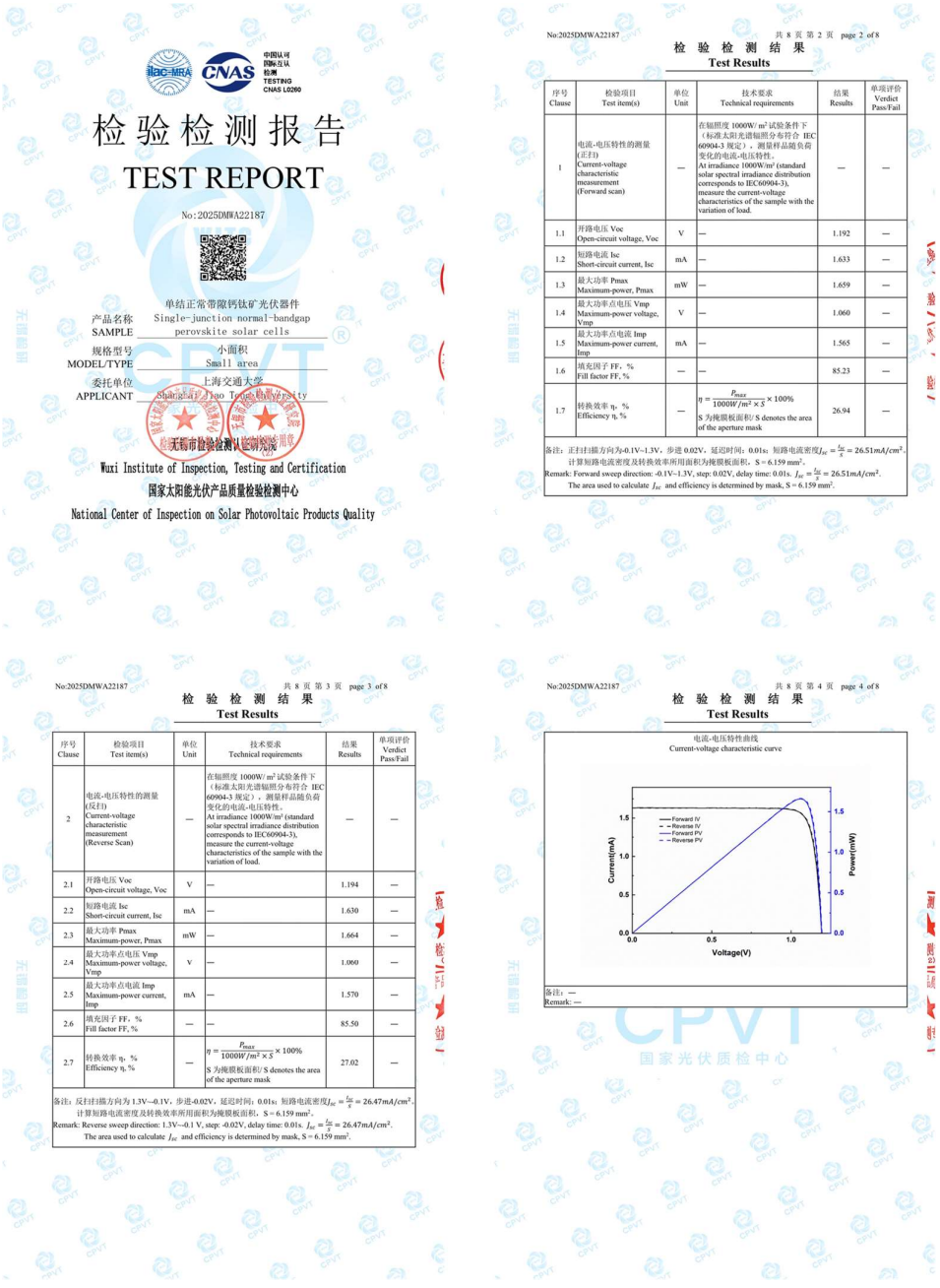

检验检测报告
TEST REPORT

No:2025DMWA22187

产品名称 SAMPLE: 单结正常带隙钙钛矿光伏器件 Single-junction normal-bandgap perovskite solar cells

规格型号 MODEL/TYPE: 小面积 Small area

委托单位 APPLICANT: 上海交通大学 Shanghai Jiao Tong University

无锡市检验检测认证研究院

Wuxi Institute of Inspection, Testing and Certification

国家太阳能光伏产品质量检验检测中心

National Center of Inspection on Solar Photovoltaic Products Quality

No:2025DMWA22187 共 8 页 第 2 页 page 2 of 8

检 验 检 测 结 果
Test Results

序号 Clause	检验项目 Test item(s)	单位 Unit	技术要求 Technical requirements	结果 Results	单项评价 Verdict Pass/Fail
1	电流-电压特性的测量 (正扫) Current-voltage characteristic measurement (Forward scan)	—	在辐照度 1000W/ m² 试验条件下（标准太阳光谱辐照分布符合 IEC 60904-3 规定），测量样品随负荷变化的电流-电压特性。 At irradiance 1000W/m² (standard solar spectral irradiance distribution corresponds to IEC60904-3), measure the current-voltage characteristics of the sample with the variation of load.	—	—
1.1	开路电压 Voc Open-circuit voltage, Voc	V	—	1.192	—
1.2	短路电流 Isc Short-circuit current, Isc	mA	—	1.633	—
1.3	最大功率 Pmax Maximum-power, Pmax	mW	—	1.659	—
1.4	最大功率点电压 Vmp Maximum-power voltage, Vmp	V	—	1.060	—
1.5	最大功率点电流 Imp Maximum-power current, Imp	mA	—	1.565	—
1.6	填充因子 FF，% Fill factor FF, %	—	—	85.23	—
1.7	转换效率 η，% Efficiency η, %	—	$\eta = \frac{P_{max}}{1000W/m^2 \times S} \times 100\%$ S 为掩膜板面积/ S denotes the area of the aperture mask	26.94	—

备注：正扫扫描方向为-0.1V--1.3V，步进 0.02V，延迟时间：0.01s；短路电流密度 $J_{sc} = \frac{I_{sc}}{s} = 26.51mA/cm^2$，计算短路电流密度及转换效率所用面积为掩膜板面积，S = 6.159 mm²。

Remark: Forward sweep direction: -0.1V--1.3V, step: 0.02V, delay time: 0.01s. $J_{sc} = \frac{I_{sc}}{s} = 26.51mA/cm^2$. The area used to calculate J_{sc} and efficiency is determined by mask, S = 6.159 mm².

No:2025DMWA22187 共 8 页 第 3 页 page 3 of 8

检 验 检 测 结 果
Test Results

序号 Clause	检验项目 Test item(s)	单位 Unit	技术要求 Technical requirements	结果 Results	单项评价 Verdict Pass/Fail
2	电流-电压特性的测量 (反扫) Current-voltage characteristic measurement (Reverse Scan)	—	在辐照度 1000W/ m² 试验条件下（标准太阳光谱辐照分布符合 IEC 60904-3 规定），测量样品随负荷变化的电流-电压特性。 At irradiance 1000W/m² (standard solar spectral irradiance distribution corresponds to IEC60904-3), measure the current-voltage characteristics of the sample with the variation of load.	—	—
2.1	开路电压 Voc Open-circuit voltage, Voc	V	—	1.194	—
2.2	短路电流 Isc Short-circuit current, Isc	mA	—	1.630	—
2.3	最大功率 Pmax Maximum-power, Pmax	mW	—	1.664	—
2.4	最大功率点电压 Vmp Maximum-power voltage, Vmp	V	—	1.060	—
2.5	最大功率点电流 Imp Maximum-power current, Imp	mA	—	1.570	—
2.6	填充因子 FF，% Fill factor FF, %	—	—	85.50	—
2.7	转换效率 η，% Efficiency η, %	—	$\eta = \frac{P_{max}}{1000W/m^2 \times S} \times 100\%$ S 为掩膜板面积/ S denotes the area of the aperture mask	27.02	—

备注：反扫扫描方向为 1.3V--0.1V，步进-0.02V，延迟时间：0.01s；短路电流密度 $J_{sc} = \frac{I_{sc}}{s} = 26.47mA/cm^2$，计算短路电流密度及转换效率所用面积为掩膜板面积，S = 6.159 mm²。

Remark: Reverse sweep direction: 1.3V--0.1 V, step: -0.02V, delay time: 0.01s. $J_{sc} = \frac{I_{sc}}{s} = 26.47mA/cm^2$. The area used to calculate J_{sc} and efficiency is determined by mask, S = 6.159 mm².

No:2025DMWA22187 共 8 页 第 4 页 page 4 of 8

检 验 检 测 结 果
Test Results

电流-电压特性曲线
Current-voltage characteristic curve

备注：—
Remark: —

Supplementary Fig. 44 *J-V* characteristics certification report of the champion device.

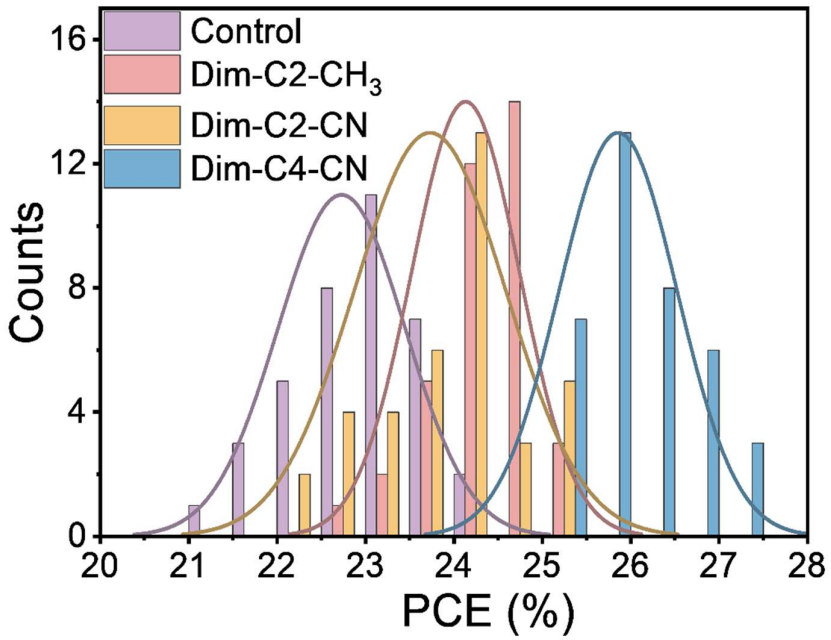

Supplementary Fig. 45 PCE distribution of the devices.

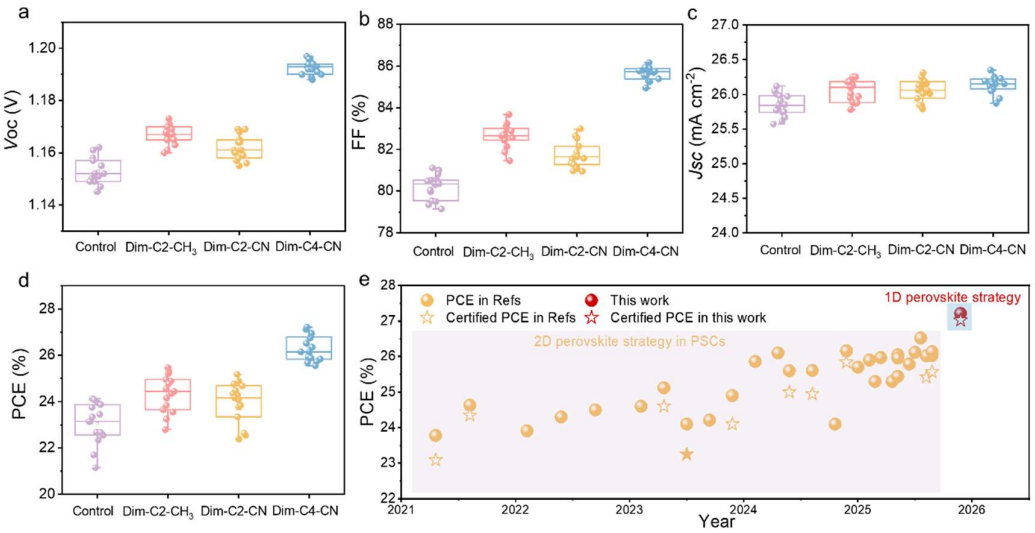

Supplementary Fig. 46 Photovoltaic performance statistics of the devices. The statistics of photovoltaic performance parameters of control and ligands-modified PSCs: (a) V_{OC}, (b) FF, (c) J_{SC} and (d) PCE. In the box plots, the central line denotes the median, the square indicates the mean, the box bounds represent the 25th and 75th percentiles, while the whiskers extend to the furthest data points within 1.5 times the interquartile range. (e) A statistical comparison of device efficiencies based on the 1D/3D perovskite strategy versus reported 2D/3D perovskite strategy.

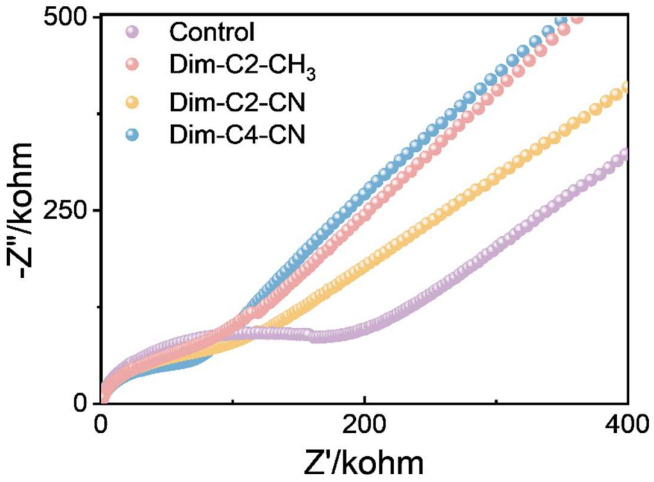

Supplementary Fig. 47 EIS measurements of reference, Dim-C2-CH_3-, Dim-C2-CN-, and Dim-C4-CN-modified perovskite devices. The EIS spectrum exhibits two distinct arcs, corresponding to the charge transport resistance (R_{ct}) in the high-frequency region and recombination resistance (R_{rec}) in the low-frequency region, respectively. Compared to the control device, the Dim-C4-CN-modified device demonstrates significantly reduced R_{ct} and enhanced R_{rec}, indicating improved charge transport efficiency and suppressed charge recombination at the interface.

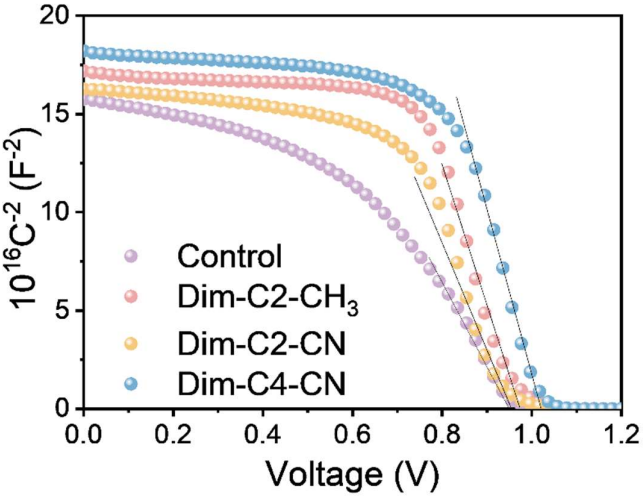

Supplementary Fig. 48 Mott-Schottky measurements of reference, Dim-C2-CH_3-, Dim-C2-CN-, and Dim-C4-CN-modified perovskite devices. The Mott-Schottky plot slope exhibits an inverse relationship with interfacial carrier density. Notably, devices modified with Dim-C2-CH3, Dim-C2-CN, and Dim-C4-CN demonstrate increased slopes compared to the control device, clearly indicating suppressed carrier recombination. More significantly, the built-in potential (V_{bi}) shows substantial enhancement from 0.94 V (control) to 0.95 V (Dim-C2-CN), 0.97 V (Dim-C2-CH_3), and 1.02 V (Dim-C4-CN), which we attribute to improved charge carrier transport and extraction efficiency. This enhancement directly correlates with the observed increase in V_{OC} for the PSCs.

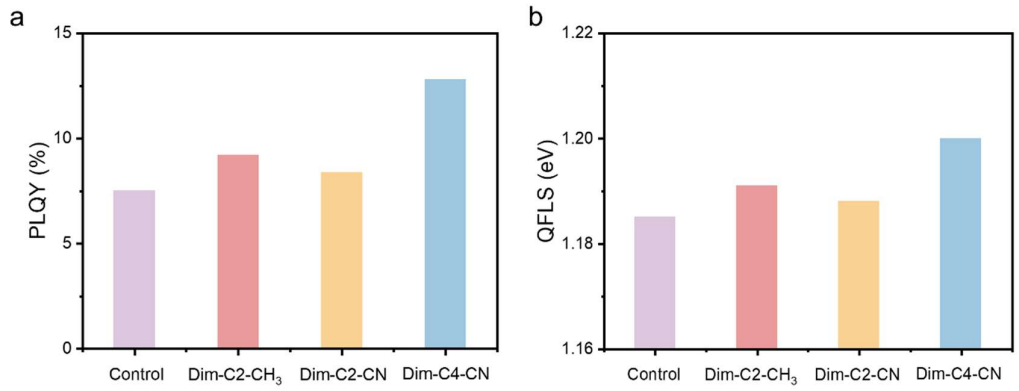

Supplementary Fig. 49 (a) PLQY values and (b) QFLS values for perovskite films.

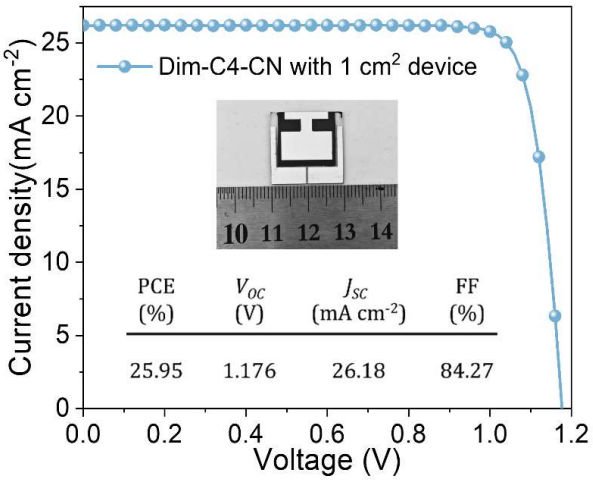

Supplementary Fig. 50 The *J-V* curves of Dim-C4-CN-modified PSCs with an effective area of 1 cm^2.

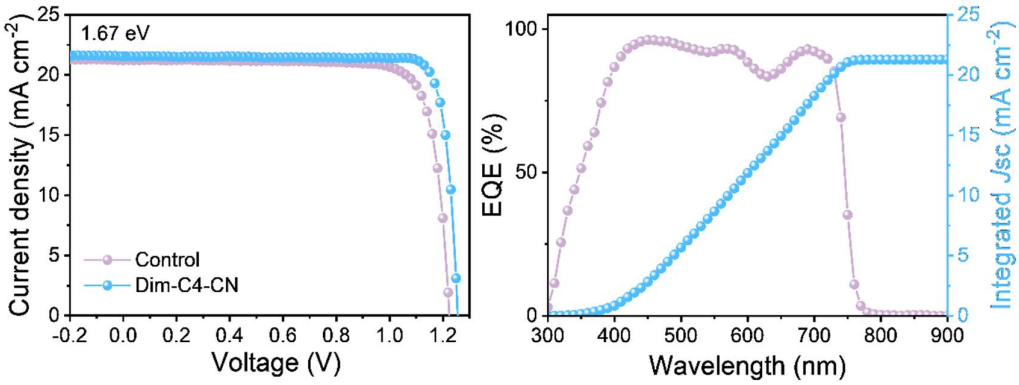

Supplementary Fig. 51 The *J-V* curves of control and Dim-C4-CN-modified 1.67 eV PSCs and EQE spectrum.

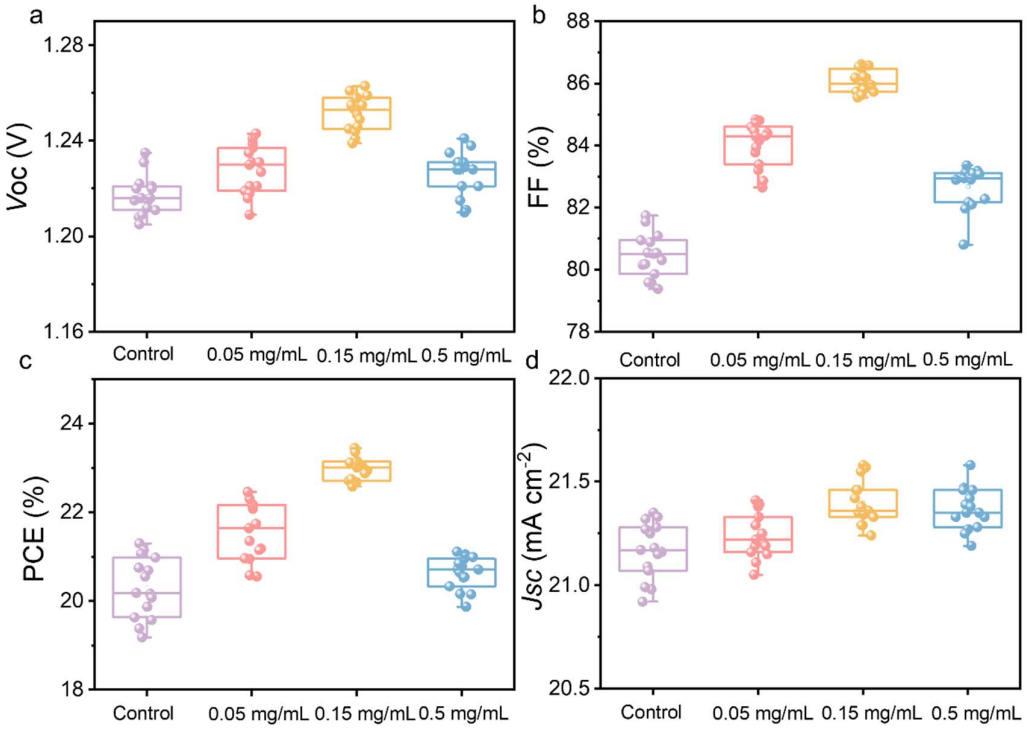

Supplementary Fig. 52 Photovoltaic performance statistics of the devices with bandgaps of 1.67 eV treated with varying concentrations of Dim-C4-CN. The statistics of photovoltaic performance parameters of control and ligands-modified PSCs: (a) V_{OC}, (b) FF, (c) PCE and (d) J_{SC}. In the box plots, the central line denotes the median, the square indicates the mean, the box bounds represent the 25th and 75th percentiles, while the whiskers extend to the furthest data points within 1.5 times the interquartile range.

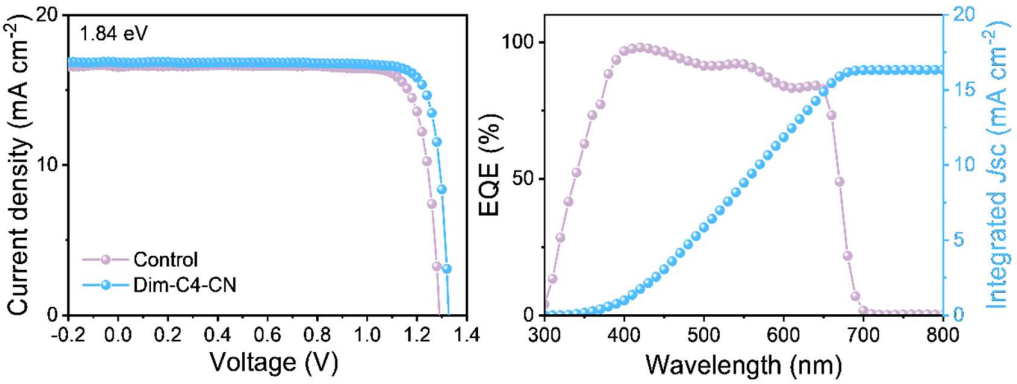

Supplementary Fig. 53 The *J-V* curves of control and Dim-C4-CN-modified 1.84 eV PSCs and EQE spectrum.

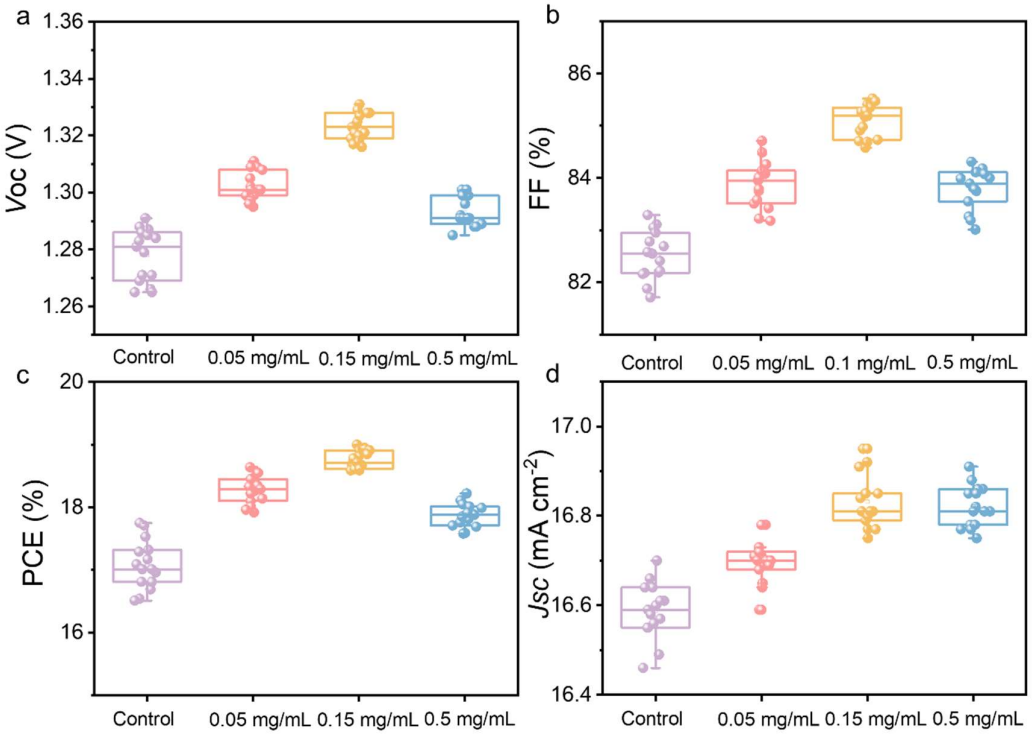

Supplementary Fig. 54 Photovoltaic performance statistics of the devices with bandgaps of 1.84 eV treated with varying concentrations of Dim-C4-CN. The statistics of photovoltaic performance parameters of control and ligands-modified PSCs: (a) V_{OC}, (b) FF, (c) PCE and (d) J_{SC}. In the box plots, the central line denotes the median, the square indicates the mean, the box bounds represent the 25th and 75th percentiles, while the whiskers extend to the furthest data points within 1.5 times the interquartile range.

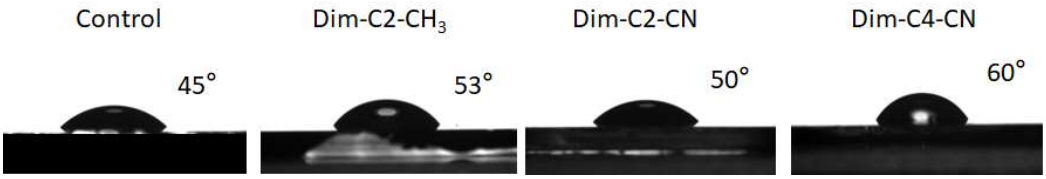

Supplementary Fig. 55 Contact angle of perovskite films.

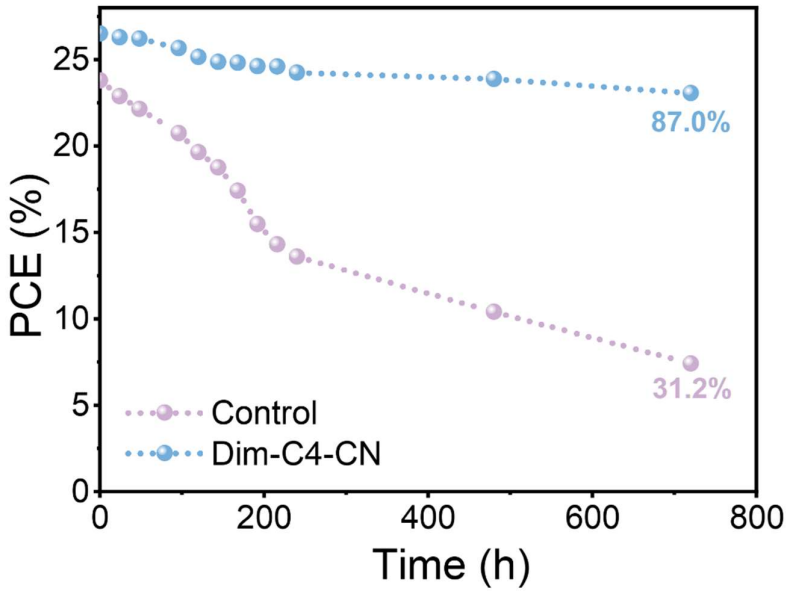

Supplementary Fig. 56 Long-term stability of control and Dim-C4-CN-modified devices monitoring at 85% RH and 85 °C (ISOS-D-3).

Supplementary Table 1. Details of X-ray crystallographic parameters of (Dim-C2-CH_3)$_3$$Pb_3$$I_{4.9}$$Br_{7.1}$ single crystal.

Empirical formula	$C_{48}H_{84}Br_{7.1}I_{4.9}N_{12}Pb_3$
Formula weight	2639.85
Temperature/K	100.0
Crystal system	trigonal
Space group	R-3
a/Å	17.9466(17)
b/Å	17.9466(17)
c/Å	21.307(2)
α/°	90
β/°	90
γ/°	120
Volume/Å^3	5943.2(13)
Z	3
ρcalcg/cm^3	2.213
2Θ range for data collection/°	4.636 to 57.472
Index ranges	$-24 \le h \le 24$, $-24 \le k \le 24$, $-28 \le l \le 28$
Reflections collected	20429
Independent reflections	3419 [Rint = 0.0562, Rsigma = 0.0389]
Data/restraints/parameters	3419/0/135
Goodness-of-fit on F2	1.050
Final R indexes [I>=2σ (I)]	R1 = 0.0293, wR2 = 0.0623

Supplementary Table 2. Fractional Atomic Coordinates (×104) and Equivalent Isotropic Displacement Parameters (Å2×103) for (Dim-C2-CH_3)$_3$$Pb_3I_{4.9}Br_{7.1}$. Ueq is defined as 1/3 of the trace of the orthogonalised UIJ tensor.

Atom	***x***	***y***	***z***	**U(eq)**
$Pb^{(1)}$	10000	10000	5000	31.18(9)
$Pb^{(2)}$	10000	10000	3008.7(2)	36.31(9)
$I^{(1)}$	8721(12)	8689(9)	4083(9)	36.4(14)
$I^{(2)}$	9592(2)	8416(2)	2265(2)	52.3(6)
$Br^{(1)}$	8605(3)	8682(3)	4146(2)	45.8(8)
$Br^{(2)}$	9529(6)	8346(7)	2348(6)	51.8(17)
$N^{(1)}$	6020(2)	6176(2)	2431.1(17)	41.2(8)
$C^{(1)}$	5778(3)	6641(3)	2765(2)	46.4(11)
$N^{(2)}$	6468(2)	7265(2)	3055.0(19)	46.2(9)
$C^{(3)}$	7176(3)	7198(3)	2887(2)	49.7(11)
$C^{(4)}$	6893(3)	6512(3)	2513(2)	48.3(11)
$C^{(5)}$	6461(3)	7904(3)	3493(2)	50.1(11)
$C^{(6)}$	5442(3)	5398(3)	2081(2)	49.6(11)
$C^{(7)}$	5130(3)	4591(3)	2473(2)	55.7(12)
$C^{(8)}$	4500(4)	3797(4)	2120(3)	73.2(17)
$C^{(9)}$	4166(5)	2977(4)	2484(4)	97(3)

Supplementary Table 3. Anisotropic Displacement Parameters (Å2×103) for (Dim-C2-CH_3)$_3$$Pb_3I_{4.9}Br_{7.1}$. The Anisotropic displacement factor exponent takes the form: -2π2[h2a*2U11+2hka*b*U12+…].

Atom	U11	U22	U33	U23	U13	U12
Pb(1)	32.62(12)	32.62(12)	28.31(18)	0	0	16.31(6)
Pb(2)	36.77(11)	36.77(11)	35.38(15)	0	0	18.38(5)
I(1)	31(3)	34.7(19)	42(3)	-6.1(14)	-3(2)	15.4(18)
I(2)	56.9(11)	50.6(8)	56.8(10)	-13.8(10)	-7.9(8)	32.4(8)
Br(1)	35.6(12)	47.8(7)	50.0(13)	-12.0(6)	-10.3(9)	17.8(6)
Br(2)	36.2(15)	56(2)	63(4)	3.1(14)	-1.6(15)	22.5(12)
N(1)	40.4(19)	41.7(19)	40.1(19)	-1.8(16)	0.2(15)	19.4(16)
C(1)	40(2)	44(2)	55(3)	-11(2)	-8(2)	21(2)
N(2)	40(2)	41(2)	53(2)	-7.5(17)	-4.9(17)	16.8(17)
C(3)	34(2)	51(3)	59(3)	0(2)	0(2)	17(2)
C(4)	39(2)	57(3)	52(3)	1(2)	4(2)	27(2)
C(5)	46(3)	46(3)	49(3)	6(2)	8(2)	16(2)
C(6)	53(3)	48(3)	48(3)	-15(2)	-9(2)	25(2)
C(7)	55(3)	50(3)	52(3)	-12(2)	-2(2)	20(2)
C(8)	72(4)	60(3)	82(4)	-27(3)	-10(3)	29(3)
C(9)	98(5)	47(3)	119(6)	-8(4)	29(5)	15(3)

Supplementary Table 4. Bond Lengths for (Dim-C2-CH_3)$_3$$Pb_3I_{4.9}Br_{7.1}$.

Atom	Atom	Length/Å	Atom	Atom	Length/Å
Pb(1)	I(1)	3.037(18)	Pb(2)	I(2)1	3.008(2)
Pb(1)	I(1)1	3.037(18)	Pb(2)	I(2)2	3.008(2)
Pb(1)	I(1)2	3.037(18)	Pb(2)	Br(2)	3.000(8)
Pb(1)	I(1)3	3.037(18)	Pb(2)	Br(2)2	3.000(9)
Pb(1)	I(1)4	3.037(18)	Pb(2)	Br(2)1	3.000(8)
Pb(1)	I(1)5	3.037(18)	N(1)	C(1)	1.326(6)
Pb(1)	Br(1)	3.041(5)	N(1)	C(4)	1.380(6)
Pb(1)	Br(1)5	3.041(5)	N(1)	C(6)	1.461(6)
Pb(1)	Br(1)1	3.041(5)	C(1)	N(2)	1.335(6)
Pb(1)	Br(1)3	3.041(5)	N(2)	C(3)	1.381(6)
Pb(1)	Br(1)4	3.041(5)	N(2)	C(5)	1.484(6)
Pb(1)	Br(1)2	3.041(5)	C(3)	C(4)	1.334(7)
Pb(2)	I(1)	3.262(17)	C(5)	C(5)6	1.499(9)
Pb(2)	I(1)1	3.262(17)	C(6)	C(7)	1.516(7)
Pb(2)	I(1)2	3.262(17)	C(7)	C(8)	1.505(7)
Pb(2)	I(2)	3.008(2)	C(8)	C(9)	1.498(9)

Supplementary Table 5. Bond Angles for $(Dim\text{-}C2\text{-}CH_3)_3Pb_3I_{4.9}Br_{7.1}$.

Atom	Atom	Atom	Angle/°	Atom	Atom	Atom	Angle/°
I(1)	Pb(1)	I(1)1	83.0(5)	I(2)	Pb(2)	I(1)1	162.4(3)
I(1)2	Pb(1)	I(1)1	180	I(2)1	Pb(2)	I(1)1	86.4(3)
I(1)3	Pb(1)	I(1)1	97.0(5)	I(2)5	Pb(2)	I(1)	162.4(3)
I(1)2	Pb(1)	I(1)4	83.0(5)	I(2)5	Pb(2)	I(1)1	102.6(3)
I(1)1	Pb(1)	I(1)4	97.0(5)	I(2)1	Pb(2)	I(1)	102.6(3)
I(1)	Pb(1)	I(1)4	97.0(5)	I(2)	Pb(2)	I(1)	86.4(3)
I(1)3	Pb(1)	I(1)4	83.0(5)	I(2)1	Pb(2)	I(2)5	94.82(14)
I(1)5	Pb(1)	I(1)4	180	I(2)1	Pb(2)	I(2)	94.82(14)
I(1)1	Pb(1)	Br(1)1	4.6(5)	I(2)5	Pb(2)	I(2)	94.82(14)
I(1)2	Pb(1)	Br(1)4	87.6(3)	Br(2)5	Pb(2)	I(1)1	101.0(4)
I(1)1	Pb(1)	Br(1)4	92.4(3)	Br(2)5	Pb(2)	I(1)5	82.3(4)
I(1)5	Pb(1)	Br(1)1	83.3(4)	Br(2)	Pb(2)	I(1)5	101.0(4)
I(1)3	Pb(1)	Br(1)1	92.4(3)	Br(2)1	Pb(2)	I(1)5	158.4(4)
I(1)2	Pb(1)	Br(1)1	175.4(5)	Br(2)	Pb(2)	I(1)1	158.4(4)
I(1)4	Pb(1)	Br(1)1	96.7(4)	Br(2)1	Pb(2)	I(1)1	82.3(4)
I(1)4	Pb(1)	Br(1)4	4.6(5)	Br(2)1	Pb(2)	I(2)5	96.3(2)
I(1)5	Pb(1)	Br(1)4	175.4(5)	Br(2)1	Pb(2)	I(2)1	4.1(4)
I(1)	Pb(1)	Br(1)4	96.7(4)	Br(2)5	Pb(2)	I(2)1	98.5(2)
I(1)	Pb(1)	Br(1)1	87.6(3)	Br(2)	Pb(2)	I(2)1	96.3(2)
I(1)3	Pb(1)	Br(1)4	83.3(4)	Br(2)5	Pb(2)	I(2)5	4.1(4)
Br(1)	Pb(1)	Br(1)2	92.11(13)	Br(2)	Pb(2)	I(2)5	98.5(2)
Br(1)3	Pb(1)	Br(1)1	92.11(13)	Br(2)1	Pb(2)	Br(2)5	99.8(4)
Br(1)	Pb(1)	Br(1)5	87.89(13)	Br(2)5	Pb(2)	Br(2)	99.8(4)
Br(1)	Pb(1)	Br(1)1	87.89(13)	Br(2)1	Pb(2)	Br(2)	99.8(4)
Br(1)5	Pb(1)	Br(1)2	92.11(13)	Pb(1)	I(1)	Pb(2)	84.6(4)
Br(1)3	Pb(1)	Br(1)4	87.89(13)	C(1)	N(1)	C(4)	108.3(4)
Br(1)4	Pb(1)	Br(1)2	87.89(13)	C(1)	N(1)	C(6)	125.2(4)
Br(1)3	Pb(1)	Br(1)5	92.11(13)	C(4)	N(1)	C(6)	126.3(4)
Br(1)2	Pb(1)	Br(1)1	180	N(1)	C(1)	N(2)	108.5(4)
Br(1)	Pb(1)	Br(1)4	92.11(13)	C(1)	N(2)	C(3)	108.4(4)
Br(1)3	Pb(1)	Br(1)2	87.89(13)	C(1)	N(2)	C(5)	125.2(4)
Br(1)5	Pb(1)	Br(1)1	87.89(13)	C(3)	N(2)	C(5)	126.4(4)
Br(1)4	Pb(1)	Br(1)5	180	C(4)	C(3)	N(2)	107.0(4)
Br(1)	Pb(1)	Br(1)3	180	C(3)	C(4)	N(1)	107.7(4)
Br(1)4	Pb(1)	Br(1)1	92.11(13)	N(2)	C(5)	C(5)6	108.5(5)
I(1)5	Pb(2)	I(1)1	76.2(5)	N(1)	C(6)	C(7)	112.2(4)
I(1)5	Pb(2)	I(1)	76.2(5)	C(8)	C(7)	C(6)	111.9(5)
I(1)1	Pb(2)	I(1)	76.2(5)	C(9)	C(8)	C(7)	114.4(6)

Supplementary Table 6. Torsion Angles for (Dim-C2-CH_3)$_3$$Pb_3I_{4.9}Br_{7.1}$.

A	B	C	D	Angle/°
N(1)	C(1)	N(2)	C(3)	1.2(5)
N(1)	C(1)	N(2)	C(5)	-177.6(4)
N(1)	C(6)	C(7)	C(8)	177.1(4)
C(1)	N(1)	C(4)	C(3)	-1.6(5)
C(1)	N(1)	C(6)	C(7)	-90.6(6)
C(1)	N(2)	C(3)	C(4)	-2.2(6)
C(1)	N(2)	C(5)	C(5)1	-108.1(6)
N(2)	C(3)	C(4)	N(1)	2.3(6)
C(3)	N(2)	C(5)	C(5)1	73.3(7)
C(4)	N(1)	C(1)	N(2)	0.2(5)
C(4)	N(1)	C(6)	C(7)	83.9(6)
C(5)	N(2)	C(3)	C(4)	176.6(4)
C(6)	N(1)	C(1)	N(2)	175.6(4)
C(6)	N(1)	C(4)	C(3)	-176.9(4)
C(6)	C(7)	C(8)	C(9)	-179.7(5)

Supplementary Table 7. Hydrogen Atom Coordinates (Å×104) and Isotropic Displacement Parameters (Å2×103) for (Dim-C2-CH_3)$_3$$Pb_3$$I_{4.9}$$Br_{7.1}$.

Atom	x	y	z	U(eq)
H(1)	5208.59	6547.47	2793.27	56
H(3)	7754.15	7570.27	3012.68	60
H(4)	7231.96	6294.94	2336.07	58
H(5A)	6783.59	7939.22	3879.84	60
H(5B)	5862.14	7728.49	3612.14	60
H(6A)	5745.31	5357.56	1705.57	60
H(6B)	4939.03	5437.98	1934.86	60
H(7A)	5630.16	4533.95	2599.96	67
H(7B)	4852.53	4643.25	2858.51	67
H(8A)	4007.27	3862.96	1989.06	88
H(8B)	4782.87	3751	1734.03	88
H(9A)	3789.74	2489.01	2215.33	146
H(9B)	3838.9	2993.17	2847.52	146
H(9C)	4649.44	2913.76	2628.66	146

Supplementary Table 8. Atomic Occupancy for $(Dim\text{-}C2\text{-}CH_3)_3Pb_3I_{4.9}Br_{7.1}$.

Atom	Occupancy
I(1)	0.152(5)
Br(2)	0.336(5)
I(2)	0.664(5)
Br(1)	0.848(5)

Supplementary Table 9. Crystal data and structure refinement for Dim-C2-CN(PbI_3)$_2$.

Identification code	A
Empirical formula	$C_{16}H_{22}I_6N_6Pb_2$
Formula weight	1474.17
Temperature/K	193
Crystal system	monoclinic
Space group	C2/c
a/Å	12.342(3)
b/Å	21.024(6)
c/Å	8.1132(18)
α/°	90
β/°	129.456(8)
γ/°	90
Volume/Å3	1625.3(7)
Z	2
ρcalcg/cm3	3.012
μ/mm-1	16.058
F(000)	1284
Crystal size/mm3	0.13 × 0.12 × 0.1
Radiation	MoKα (λ = 0.71073)
2Θ range for data collection/°	5.384 to 54.91
Index ranges	-15 ≤ h ≤ 15, -27 ≤ k ≤ 26, -10 ≤ l ≤ 10
Reflections collected	6883
Independent reflections	1860 [Rint = 0.0634, Rsigma = 0.0515]
Data/restraints/parameters	1860/343/243
Goodness-of-fit on F2	1.053
Final R indexes [I>=2σ (I)]	R1 = 0.0720, wR2 = 0.2014
Final R indexes [all data]	R1 = 0.0968, wR2 = 0.2243
Largest diff. peak/hole / e Å-3	2.24/-1.72

Supplementary Table 10. Fractional Atomic Coordinates ($\times 10^4$) and Equivalent Isotropic Displacement Parameters ($Å2\times 10^3$) for Dim-C2-CN$(PbI_3)_2$. Ueq is defined as 1/3 of the trace of the orthogonalised UIJ tensor.

Atom	x	y	z	U(eq)
Pb1	5000	5000	5000	64.9(6)
I2	5000	3799(3)	2500	65(3)
I3	2536(16)	5511(7)	100(20)	85(2)
Pb1A	5920(40)	4994(10)	5960(40)	64.9(6)
I3A	2940(20)	5647(9)	500(30)	91(3)
I2A	5570(30)	3800(6)	3170(40)	63(4)
C9	10270(110)	3930(40)	6890(140)	94(9)
C10	10620(50)	3100(30)	5700(80)	95(9)
N5	10120(40)	2590(20)	4410(70)	93(9)
N4	9530(60)	3430(30)	5280(110)	97(9)
C13	10890(60)	2130(30)	4160(90)	97(10)
C12	8660(40)	2610(30)	3080(90)	96(9)
C11	8350(50)	3050(30)	4000(110)	95(9)
C6	11430(50)	3350(30)	10310(110)	103(10)
C8	9260(80)	3980(40)	7550(110)	96(9)
N3	10030(50)	3500(20)	9210(80)	101(9)
C7	9530(50)	3100(30)	9880(100)	103(9)
N2	10550(70)	2700(30)	11350(90)	105(9)
C5	11790(50)	2900(30)	11810(100)	103(10)
C4	10430(90)	2310(20)	12710(110)	111(10)
C14	10450(70)	2000(40)	1990(80)	98(10)
C3	10740(60)	2640(40)	14610(80)	110(10)
C15	11520(70)	2200(40)	1780(110)	105(11)
C2	9460(70)	2890(40)	14200(160)	108(11)
C16	11010(90)	2720(40)	180(140)	106(11)
C1	9710(110)	3500(40)	15370(190)	105(12)
N6	11640(80)	3070(40)	-320(120)	93(13)
N1	9530(80)	4050(30)	15870(130)	88(14)

Supplementary Table 11. Anisotropic Displacement Parameters (Å2×103) for Dim-C2-CN(PbI_3)$_2$. The Anisotropic displacement factor exponent takes the form: -2 2[h2a*2U11+2hka*b*U12+…].

Atom	U11	U22	U33	U23	U13	U12
Pb1	96.5(17)	71.2(7)	55.9(9)	2.3(5)	62.1(12)	2.7(6)
I2	77(7)	68.7(19)	60(6)	0	49(6)	0
I3	97(4)	106(4)	84(3)	4(3)	72(3)	15(3)
Pb1A	96.5(17)	71.2(7)	55.9(9)	2.3(5)	62.1(12)	2.7(6)
I3A	109(6)	104(5)	69(4)	24(3)	61(4)	24(4)
I2A	86(9)	56(4)	50(7)	-1(4)	44(6)	8(5)
C9	96(10)	98(10)	95(10)	1(7)	64(7)	1(7)
C10	96(10)	96(10)	95(10)	1(7)	62(7)	1(7)
N5	96(10)	95(10)	94(10)	0(6)	63(7)	2(6)
N4	97(9)	98(9)	96(9)	2(6)	62(7)	0(6)
C13	100(10)	98(11)	96(10)	0(7)	63(7)	2(7)
C12	96(10)	95(10)	97(10)	0(7)	61(7)	0(7)
C11	96(10)	96(10)	96(10)	0(7)	62(7)	2(7)
C6	102(10)	104(11)	103(10)	-1(7)	66(7)	1(7)
C8	98(10)	100(10)	96(10)	-2(7)	65(7)	3(7)
N3	102(10)	103(10)	100(9)	-2(6)	65(7)	3(6)
C7	103(10)	104(10)	102(10)	0(7)	66(7)	2(7)
N2	106(10)	106(10)	105(10)	1(6)	67(7)	0(6)
C5	104(10)	105(11)	103(11)	0(7)	67(7)	0(7)
C4	108(11)	109(11)	109(11)	1(7)	67(7)	1(7)
C14	102(11)	99(11)	97(11)	-2(7)	65(8)	3(7)
C3	109(11)	109(11)	109(11)	2(7)	68(8)	-1(7)
C15	105(12)	104(12)	103(12)	-1(7)	65(8)	1(7)
C2	108(12)	109(12)	107(12)	3(7)	68(8)	-2(7)
C16	107(13)	107(13)	104(13)	-2(8)	67(8)	0(8)
C1	106(13)	107(13)	104(13)	3(8)	67(9)	-3(8)
N6	112(18)	114(19)	87(17)	-10(14)	79(13)	2(14)
N1	94(18)	97(18)	89(17)	2(14)	66(13)	2(14)

Supplementary Table 12. Bond Lengths for Dim-C2-CN$(PbI_3)_2$.

Atom	Atom	Length/Å	Atom	Atom	Length/Å
Pb1	I21	3.239(4)	N4	C11	1.393(10)
Pb1	I2	3.239(4)	C13	C14	1.503(11)
Pb1	I31	3.294(12)	C12	C11	1.386(10)
Pb1	I32	3.272(9)	C6	N3	1.383(9)
Pb1	I3	3.294(12)	C6	C5	1.378(9)
Pb1	I33	3.272(9)	C8	N3	1.451(11)
Pb1A	Pb1A1	1.77(8)	N3	C7	1.343(9)
Pb1A	I3A1	2.63(2)	C7	N2	1.345(9)
Pb1A	I3A2	2.72(2)	N2	C5	1.386(10)
Pb1A	I2A	3.22(3)	N2	C4	1.451(11)
Pb1A	I2A3	3.29(3)	C4	C3	1.502(11)
I2A	I2A2	1.10(6)	C14	C15	1.499(11)
C9	N4	1.451(11)	C3	C2	1.498(11)
C9	C8	1.64(11)	C15	C16	1.499(11)
C10	N5	1.343(9)	C2	C1	1.501(11)
C10	N4	1.348(9)	C16	N6	1.300(8)
N5	C13	1.453(11)	C1	N1	1.300(8)
N5	C12	1.391(10)			

Supplementary Table 13. Bond Angles for Dim-C2-CN(PbI_3)$_2$.

Atom	Atom	Atom	Angle/˚
I21	Pb1	I2	180
I2	Pb1	I32	97.4(2)
I21	Pb1	I32	82.6(2)
I2	Pb1	I3	82.3(2)
I21	Pb1	I31	82.3(2)
I21	Pb1	I33	97.4(2)
I2	Pb1	I31	97.7(2)
I2	Pb1	I33	82.6(2)
I21	Pb1	I3	97.7(2)
I33	Pb1	I3	91.3(5)
I3	Pb1	I31	180
I33	Pb1	I31	88.7(5)
I32	Pb1	I31	91.3(5)
I32	Pb1	I33	180.0(5)
I32	Pb1	I3	88.7(5)
Pb1	I2	Pb13	77.55(12)
Pb13	I3	Pb1	76.3(2)
Pb1A1	Pb1A	I2A	82.4(14)
Pb1A1	Pb1A	I2A2	85.6(14)
I3A3	Pb1A	I2A2	97.7(8)
I3A3	Pb1A	I2A	88.0(7)
I3A1	Pb1A	I2A2	87.9(7)
I3A1	Pb1A	I2A	96.2(8)
I2A	Pb1A	I2A2	167.9(16)
I2A3	I2A	Pb1A	102(2)
N4	C9	C8	100(6)
N5	C10	N4	109.5(7)
C10	N5	C13	128.6(12)
C10	N5	C12	107.4(7)
C12	N5	C13	123.5(12)
C10	N4	C9	101(6)
C10	N4	C11	106.6(8)
C11	N4	C9	148(5)
N5	C13	C14	120(5)
C11	C12	N5	105.8(8)
C12	C11	N4	105.4(9)
C5	C6	N3	107.1(6)
N3	C8	C9	94(5)
C6	N3	C8	124.3(12)
C7	N3	C6	107.8(6)
C7	N3	C8	127.8(12)
N3	C7	N2	109.6(7)

C7	N2	C5	107.6(7)
C7	N2	C4	122(5)
C5	N2	C4	126(5)
C6	C5	N2	106.8(7)
N2	C4	C3	115.8(12)
C15	C14	C13	112.9(11)
C2	C3	C4	113.1(11)
C16	C15	C14	113.1(11)
C3	C2	C1	112.9(11)
N6	C16	C15	132(7)
N1	C1	C2	162(10)

Supplementary Table 14. Torsion Angles for Dim-C2-CN(PbI_3)$_2$.

A	B	C	D	Angle/°
C9	N4	C11	C12	-171(9)
C9	C8	N3	C6	26(4)
C9	C8	N3	C7	-150(5)
C10	N5	C13	C14	-126(5)
C10	N5	C12	C11	-15(4)
C10	N4	C11	C12	-22(4)
N5	C10	N4	C9	177(2)
N5	C10	N4	C11	13(4)
N5	C13	C14	C15	115(6)
N5	C12	C11	N4	23(4)
N4	C9	C8	N3	90(5)
N4	C10	N5	C13	173(4)
N4	C10	N5	C12	1(4)
C13	N5	C12	C11	173(4)
C13	C14	C15	C16	-116(8)
C12	N5	C13	C14	45(6)
C6	N3	C7	N2	-1(5)
C8	C9	N4	C10	-141(5)
C8	C9	N4	C11	9(12)
C8	N3	C7	N2	176(3)
N3	C6	C5	N2	10(4)
N3	C7	N2	C5	7(6)
N3	C7	N2	C4	166(4)
C7	N2	C5	C6	-10(5)
C7	N2	C4	C3	-81(7)
N2	C4	C3	C2	95(8)
C5	C6	N3	C8	177(2)
C5	C6	N3	C7	-6(4)
C5	N2	C4	C3	75(8)
C4	N2	C5	C6	-169(4)
C4	C3	C2	C1	-146(8)
C14	C15	C16	N6	173(11)
C3	C2	C1	N1	152(34)

Supplementary Table 15. Hydrogen Atom Coordinates (Å×10^4) and Isotropic Displacement Parameters (Å2×10^3) for Dim-C2-CN(PbI_3)$_2$.

Atom	x	y	z	U(eq)
H9A	10297.94	4333.33	6294.48	113
H9B	11238.46	3798.01	8114.61	113
H10	11579.94	3201.66	6759.17	114
H13A	10873.15	1720.2	4742.45	117
H13B	11879.26	2272.12	5082.63	117
H12	8016.66	2378.95	1797.14	116
H11	7503.54	3081.77	3794.37	114
H6	12029.05	3531.88	10079.05	123
H8A	9296.49	4402.35	8104.14	115
H8B	8280.9	3853.85	6369.11	115
H7	8595.16	3101.8	9385.55	123
H5	12707.35	2752.69	12943.33	124
H4A	11077.85	1946.49	13219.88	133
H4B	9465.1	2141.15	11825.99	133
H14A	10273.8	1536.12	1693.5	118
H14B	9555.56	2222.8	899.2	118
H3A	11224.48	2340.25	15820.67	132
H3B	11393.8	3000.56	15025.56	132
H15A	12372.73	2349.69	3194.1	125
H15B	11790.74	1830.26	1363.54	125
H2A	9109.01	2567.65	14654.18	130
H2B	8715.05	2962.45	12652.56	130

Supplementary Table 16. Atomic Occupancy for Dim-C2-CN(PbI_3)$_2$.

Atom	Occupancy	Atom	Occupancy	Atom	Occupancy
Pb1	0.921(6)	I2	0.71(4)	I3	0.56(4)
Pb1A	0.040(3)	I3A	0.44(4)	I2A	0.146(19)
C9	0.25	H9A	0.25	H9B	0.25
C10	0.25	H10	0.25	N5	0.25
N4	0.25	C13	0.25	H13A	0.25
H13B	0.25	C12	0.25	H12	0.25
C11	0.25	H11	0.25	C6	0.25
H6	0.25	C8	0.25	H8A	0.25
H8B	0.25	N3	0.25	C7	0.25
H7	0.25	N2	0.25	C5	0.25
H5	0.25	C4	0.25	H4A	0.25
H4B	0.25	C14	0.25	H14A	0.25
H14B	0.25	C3	0.25	H3A	0.25
H3B	0.25	C15	0.25	H15A	0.25
H15B	0.25	C2	0.25	H2A	0.25
H2B	0.25	C16	0.25	C1	0.25
N6	0.25	N1	0.25		

Supplementary Table 17. Crystal data and structure refinement for Dim-C2-OMe(PbI_3)$_2$.

Empirical formula	$C_8H_{13}I_3N_2OPb$
Formula weight	741.09
Temperature/K	193
Crystal system	monoclinic
Space group	C2/m
a/Å	22.100(11)
b/Å	8.108(4)
c/Å	8.974(5)
α/°	90
β/°	109.070(14)
γ/°	90
Volume/Å3	1519.8(13)
Z	4
ρcalcg/cm3	3.239
μ/mm-1	17.177
F(000)	1296
Crystal size/mm3	0.12 × 0.08 × 0.04
Radiation	MoKα (λ = 0.71073)
2Θ range for data collection/°	3.9 to 50.69
Index ranges	-25 ≤ h ≤ 26, -9 ≤ k ≤ 9, -10 ≤ l ≤ 9
Reflections collected	4353
Independent reflections	1483 [Rint = 0.0748, Rsigma = 0.0786]
Data/restraints/parameters	1483/322/232
Goodness-of-fit on F2	1.124
Final R indexes [I>=2σ (I)]	R1 = 0.1102, wR2 = 0.2265
Final R indexes [all data]	R1 = 0.1544, wR2 = 0.2587
Largest diff. peak/hole / e Å-3	2.88/-1.60

Supplementary Table 18. Fractional Atomic Coordinates (×104) and Equivalent Isotropic Displacement Parameters (Å2×103) for Dim-C2-OMe$(PbI_3)_2$. Ueq is defined as 1/3 of the trace of the orthogonalised UIJ tensor.

Atom	x	y	z	U(eq)
Pb1	2500	7500	10000	64.3(7)
I1	1289.6(19)	10000	9136(5)	72.0(11)
I2	3116(2)	10000	12897(5)	80.7(12)
I3	3026.2(19)	10000	7934(5)	75.7(11)
Pb1A	2520(30)	7500(70)	8190(70)	64.3(7)
I1A	1310(40)	10000	6860(90)	72.0(11)
I2A	2970(40)	10000	10840(90)	80.7(12)
I3A	1890(40)	5000	5080(90)	75.7(11)
O1	4660(30)	3550(90)	7240(80)	58(9)
O2	4710(30)	16790(90)	7810(90)	60(9)
N1	4030(20)	6760(60)	6100(70)	58(7)
N2	4830(30)	8360(70)	7410(70)	59(7)
N3	4980(30)	11870(60)	7680(70)	60(7)
N4	4180(30)	13460(80)	6320(80)	60(7)
C1	5120(30)	2600(150)	6860(150)	59(11)
C2	4030(30)	2990(80)	6740(100)	58(8)
C3	3620(30)	3900(60)	5320(80)	58(8)
C4	3460(20)	5630(70)	5690(110)	58(8)
C5	4350(30)	7420(90)	7500(60)	58(7)
C6	4320(40)	7300(100)	5030(60)	59(8)
C7	4840(30)	8290(100)	5870(80)	59(7)
C8	5280(40)	9090(70)	8900(60)	59(7)
C9	5510(20)	10780(70)	8650(100)	60(7)
C10	4430(40)	12580(110)	7640(70)	60(7)
C11	5090(30)	12270(110)	6270(100)	60(7)
C12	4600(40)	13350(110)	5450(80)	60(8)
C13	3620(40)	14560(90)	5550(90)	60(8)
C14	3610(30)	16090(80)	6490(110)	60(8)
C15	4160(30)	16150(80)	8020(70)	60(8)
C16	4810(50)	18500(90)	7940(160)	61(11)

Supplementary Table 19. Anisotropic Displacement Parameters (Å2×103) for Dim-C2-OMe(PbI_3)$_2$. The Anisotropic displacement factor exponent takes the form: -2π2[h2a*2U11+2hka*b*U12+…].

Atom	U11	U22	U33	U23	U13	U12
Pb1	67.6(13)	54.2(12)	70.6(13)	-0.8(10)	22.0(10)	0.5(10)
I1	72(2)	65(2)	78(2)	0	23.2(18)	0
I2	77(3)	87(3)	71(2)	0	14.4(19)	0
I3	77(3)	80(3)	77(2)	0	33.2(19)	0
Pb1A	67.6(13)	54.2(12)	70.6(13)	-0.8(10)	22.0(10)	0.5(10)
I1A	72(2)	65(2)	78(2)	0	23.2(18)	0
I2A	77(3)	87(3)	71(2)	0	14.4(19)	0
I3A	77(3)	80(3)	77(2)	0	33.2(19)	0
O1	58(10)	57(10)	60(10)	-1(6)	20(6)	-1(6)
O2	60(10)	59(10)	60(10)	0(6)	21(6)	0(6)
N1	59(8)	58(8)	59(8)	0(5)	20(5)	0(5)
N2	59(8)	58(8)	59(8)	0(5)	20(5)	0(5)
N3	60(8)	60(8)	60(8)	0(5)	20(5)	0(5)
N4	60(8)	60(8)	60(8)	0(5)	20(5)	1(5)
C1	59(14)	58(14)	61(14)	-1(11)	20(11)	-3(11)
C2	58(9)	56(9)	59(9)	0(6)	20(6)	0(6)
C3	58(9)	57(9)	59(9)	0(5)	19(6)	0(5)
C4	59(9)	58(9)	59(9)	0(5)	20(5)	-1(5)
C5	59(8)	58(8)	59(8)	0(5)	20(5)	1(5)
C6	59(9)	58(9)	59(8)	0(5)	19(5)	0(5)
C7	59(8)	58(8)	59(8)	0(5)	19(5)	1(5)
C8	59(8)	59(8)	60(8)	0(5)	20(5)	0(5)
C9	60(8)	60(8)	60(8)	0(5)	20(5)	0(5)
C10	60(8)	60(8)	60(8)	0(5)	20(5)	0(5)
C11	60(9)	61(8)	60(8)	0(5)	20(5)	1(5)
C12	60(9)	60(9)	60(8)	0(5)	20(5)	1(5)
C13	60(9)	60(9)	60(9)	0(5)	19(5)	1(5)
C14	60(9)	60(9)	60(9)	0(5)	20(6)	1(5)
C15	60(9)	60(9)	61(9)	0(6)	20(6)	1(6)
C16	61(14)	60(14)	61(14)	-1(11)	20(11)	0(11)

Supplementary Table 20. Bond Lengths for Dim-C2-OMe$(PbI_3)_2$.

Atom	Atom	Length/Å
Pb1	I11	3.242(3)
Pb1	I1	3.242(3)
Pb1	I2	3.226(3)
Pb1	I21	3.226(3)
Pb1	I3	3.211(3)
Pb1	I31	3.211(3)
Pb1A	Pb1A1	3.27(11)
Pb1A	I1A	3.25(8)
Pb1A	I2A1	2.58(8)
Pb1A	I2A	3.03(8)
Pb1A	I3A	3.36(8)
O1	C1	1.399(11)
O1	C2	1.399(11)
O2	C15	1.401(11)
O2	C16	1.402(11)
N1	C4	1.499(11)
N1	C5	1.340(10)
N1	C6	1.394(10)
N2	C5	1.340(10)
N2	C7	1.393(10)
N2	C8	1.499(11)
N3	C9	1.499(11)
N3	C10	1.340(10)
N3	C11	1.394(10)
N4	C10	1.339(10)
N4	C12	1.393(10)
N4	C13	1.498(11)
C2	C3	1.499(11)
C3	C4	1.501(11)
C6	C7	1.396(11)
C8	C9	1.500(11)
C11	C12	1.397(11)
C13	C14	1.500(11)
C14	C15	1.500(11)

Supplementary Table 21. Bond Angles for Dim-C2-OMe(PbI_3)$_2$.

Atom	Atom	Atom	Angle/˚
I1	Pb1	I11	180
I21	Pb1	I11	84.13(9)
I21	Pb1	I1	95.87(9)
I2	Pb1	I1	84.13(9)
I2	Pb1	I11	95.87(9)
I21	Pb1	I2	180
I31	Pb1	I11	83.88(9)
I31	Pb1	I1	96.12(9)
I3	Pb1	I1	83.88(9)
I3	Pb1	I11	96.12(9)
I31	Pb1	I2	93.92(9)
I3	Pb1	I2	86.08(9)
I3	Pb1	I21	93.92(9)
I31	Pb1	I21	86.08(9)
I31	Pb1	I3	180
Pb12	I1	Pb1	77.40(10)
Pb1	I2	Pb12	77.86(10)
Pb12	I3	Pb1	78.30(9)
Pb1A1	Pb1A	I3A	133(3)
I1A	Pb1A	I3A	90(2)
I2A1	Pb1A	I1A	103(3)
I2A	Pb1A	I1A	84(2)
I2A1	Pb1A	I2A	109(2)
I2A	Pb1A	I3A	174(3)
I2A1	Pb1A	I3A	73(2)
Pb1A1	I2A	Pb1A	71(2)
Pb1A3	I2A	Pb1A	84(3)
Pb1A2	I2A	Pb1A	136(3)
C2	O1	C1	118.2(14)
C15	O2	C16	117.7(13)
C5	N1	C4	128.4(13)
C5	N1	C6	107.5(10)
C6	N1	C4	124.1(12)
C5	N2	C7	107.7(10)
C5	N2	C8	119(5)
C7	N2	C8	133(5)
C10	N3	C9	143(6)
C10	N3	C11	107.6(9)
C11	N3	C9	110(6)
C10	N4	C12	107.6(10)
C10	N4	C13	140(7)
C12	N4	C13	112(7)

O1	C2	C3	111.8(12)
C2	C3	C4	112.9(12)
N1	C4	C3	112.9(11)
N1	C5	N2	111.0(7)
N1	C6	C7	107.0(10)
N2	C7	C6	106.8(10)
N2	C8	C9	112.9(11)
N3	C9	C8	112.8(11)
N4	C10	N3	110.9(7)
N3	C11	C12	106.8(10)
N4	C12	C11	106.9(10)
N4	C13	C14	113.0(11)
C13	C14	C15	112.9(11)
O2	C15	C14	111.7(12)

Supplementary Table 22. Torsion Angles for Dim-C2-OMe(PbI_3)$_2$.

A	B	C	D	Angle/°
O1	C2	C3	C4	-74(5)
N1	C6	C7	N2	-2(5)
N2	C8	C9	N3	45(5)
N3	C11	C12	N4	-5(6)
N4	C13	C14	C15	-2(11)
C1	O1	C2	C3	-102(9)
C2	C3	C4	N1	70(4)
C4	N1	C5	N2	179.5(13)
C4	N1	C6	C7	-179(3)
C5	N1	C4	C3	-111(5)
C5	N1	C6	C7	1(4)
C5	N2	C7	C6	1(4)
C5	N2	C8	C9	-144(4)
C6	N1	C4	C3	69(6)
C6	N1	C5	N2	-1(2)
C7	N2	C5	N1	0(2)
C7	N2	C8	C9	44(8)
C8	N2	C5	N1	-175(4)
C8	N2	C7	C6	174(5)
C9	N3	C10	N4	-179.9(15)
C9	N3	C11	C12	-177(4)
C10	N3	C9	C8	62(7)
C10	N3	C11	C12	4(5)
C10	N4	C12	C11	3(5)
C10	N4	C13	C14	62(12)
C11	N3	C9	C8	-116(7)
C11	N3	C10	N4	-2(3)
C12	N4	C10	N3	-1(3)
C12	N4	C13	C14	-115(9)
C13	N4	C10	N3	-178(6)
C13	N4	C12	C11	-179(5)
C13	C14	C15	O2	84(8)
C16	O2	C15	C14	89(9)

Supplementary Table 23. Hydrogen Atom Coordinates (Å×104) and Isotropic Displacement Parameters (Å2×103) for Dim-C2-OMe$(PbI_3)_2$.

Atom	x	y	z	U(eq)
H1B	5529.81	2676.93	7710.62	89
H1C	5164.91	3008.63	5877.82	89
H1A	4976.11	1449.53	6727.22	89
H2A	3846.34	3132.7	7611.84	69
H2B	4018.93	1799.68	6497.11	69
H3A	3213.79	3287.6	4840.83	69
H3B	3843.43	3953.32	4530.09	69
H4A	3122.18	6079.08	4759.12	70
H4B	3290.99	5590.37	6576.78	70
H5	4242.01	7257.32	8437.5	70
H6	4195.91	7040.81	3938	70
H7	5134.5	8816.82	5458.59	70
H8B	5658.13	8356.49	9312.98	71
H8A	5064.32	9158.41	9696.95	71
H9B	5716.38	11306.16	9691.06	71
H9A	5840.41	10676.36	8126.16	71
H10	4241.71	12470.68	8448.44	72
H11	5431.62	11891.8	5938.86	72
H12	4559.01	13891.08	4488.9	72
H14A	3203.72	16130.54	6718.43	72
H14B	3632.27	17066.5	5851.73	72
H15A	4035.02	16848.61	8776.74	72
H15B	4245.96	15026.65	8463.54	72
H16A	4545.04	19387.51	7298.41	91
H16B	4886.34	18739.21	9058.21	91
H16C	5214.04	18432.51	7733.61	91

Supplementary Table 24. Atomic Occupancy for Dim-C2-OMe$(PbI_3)_2$.

Atom	Occupancy
Pb1	0.95
I3	0.95
I2A	0.05
O2	0.25
N3	0.25
H1B	0.25
C2	0.25
C3	0.25
C4	0.25
C5	0.25
H6	0.25
C8	0.25
C9	0.25
C10	0.25
H11	0.25
C13	0.25
H14B	0.25
H15B	0.25
H16B	0.25
I1	0.95
Pb1A	0.025
I3A	0.05
N1	0.25
N4	0.25
H1C	0.25
H2A	0.25
H3A	0.25
H4A	0.25
H5	0.25
C7	0.25
H8B	0.25
H9B	0.25
H10	0.25
C12	0.25
C14	0.25
C15	0.25
C16	0.25
H16C	0.25
I2	0.95
I1A	0.05
O1	0.25
N2	0.25

C1	0.25
H1A	0.25
H2B	0.25
H3B	0.25
H4B	0.25
C6	0.25
H7	0.25
H8A	0.25
H9A	0.25
C11	0.25
H12	0.25
H14A	0.25
H15A	0.25
H16A	0.25

Supplementary Table 25. Crystal data and structure refinement for Dim-C4-CN(PbI_3)$_2$.

Empirical formula	$C_9H_{13}I_3N_3Pb$
Formula weight	751.11
Temperature/K	150
Crystal system	monoclinic
Space group	P21/c
a/Å	9.309(2)
b/Å	22.088(5)
c/Å	8.109(2)
α/°	90
β/°	93.262(10)
γ/°	90
Volume/Å3	1664.7(7)
Z	4
ρcalcg/cm3	2.997
μ/mm-1	15.681
F(000)	1316
Crystal size/mm3	0.27 × 0.18 × 0.09
Radiation	MoKα (λ = 0.71073)
2Θ range for data collection/°	4.382 to 52.738
Index ranges	-11 ≤ h ≤ 11, -27 ≤ k ≤ 27, -10 ≤ l ≤ 10
Reflections collected	15344
Independent reflections	3396 [Rint = 0.0794, Rsigma = 0.0675]
Data/restraints/parameters	3396/0/145
Goodness-of-fit on F2	1.038
Final R indexes [I>=2σ (I)]	R1 = 0.0492, wR2 = 0.1333
Final R indexes [all data]	R1 = 0.0574, wR2 = 0.1408
Largest diff. peak/hole / e Å-3	1.79/-2.24

Supplementary Table 26. Fractional Atomic Coordinates (×104) and Equivalent Isotropic Displacement Parameters (Å2×103) for Dim-C4-CN(PbI_3)$_2$. Ueq is defined as 1/3 of of the trace of the orthogonalised UIJ tensor.

Atom	x	y	z	U(eq)
Pb(1)	6379.4(4)	2499.8(2)	3143.2(5)	33.74(16)
I(1)	6483.0(8)	3628.6(3)	794.5(9)	43.5(2)
I(2)	3997.3(8)	2994.7(4)	5364.4(10)	50.1(2)
I(3)	8550.6(8)	3178.9(3)	5699.2(9)	46.4(2)
N(1)	2870(11)	4842(4)	2678(13)	52(2)
N(2)	1525(9)	4039(4)	2199(13)	47(2)
N(3)	2224(15)	4596(7)	-1830(30)	109(6)
C(1)	4730(20)	5265(7)	4600(20)	98(7)
C(2)	4142(16)	5229(6)	2871(18)	68(4)
C(3)	1411(17)	5017(7)	2770(20)	78(4)
C(4)	599(14)	4519(7)	2496(18)	63(4)
C(5)	2864(12)	4258(5)	2325(14)	44(2)
C(6)	1092(13)	3439(6)	1805(16)	53(3)
C(7)	629(15)	3371(6)	-23(17)	61(3)
C(8)	1832(15)	3488(6)	-1221(17)	58(3)
C(9)	2080(13)	4122(7)	-1568(18)	59(3)

Supplementary Table 27. Anisotropic Displacement Parameters (Å2×103) for Dim-C4-CN(PbI_3)$_2$. The Anisotropic displacement factor exponent takes the form: -2π2[h2a*2U11+2hka*b*U12+…].

Atom	U11	U22	U33	U23	U13	U12
Pb(1)	36.0(3)	37.4(2)	28.1(3)	0.50(13)	3.49(17)	0.34(14)
I(1)	51.6(4)	37.5(4)	42.0(4)	2.4(3)	6.8(3)	3.6(3)
I(2)	44.5(4)	63.2(5)	43.0(4)	3.7(3)	5.5(3)	11.0(3)
I(3)	44.3(4)	53.2(4)	41.8(4)	-4.8(3)	3.3(3)	-11.2(3)
N(1)	57(6)	38(5)	59(7)	-3(4)	-20(5)	-2(4)
N(2)	33(5)	54(5)	53(6)	-1(4)	0(4)	0(4)
N(3)	62(9)	85(10)	181(19)	38(11)	25(10)	9(8)
C(1)	127(15)	94(12)	71(11)	32(9)	-30(10)	-72(12)
C(2)	83(10)	58(7)	58(9)	17(6)	-25(7)	-27(7)
C(3)	68(10)	72(9)	93(12)	-7(8)	-10(8)	24(8)
C(4)	42(7)	81(9)	67(9)	-23(7)	0(6)	18(6)
C(5)	46(6)	45(6)	39(6)	-1(4)	-9(5)	4(5)
C(6)	43(6)	60(7)	55(8)	5(6)	1(5)	-14(5)
C(7)	60(8)	66(8)	58(8)	-8(6)	5(6)	-17(6)
C(8)	55(7)	58(7)	60(8)	-10(6)	5(6)	-7(6)
C(9)	36(6)	78(9)	64(9)	9(7)	4(6)	-1(6)

Supplementary Table 28. Bond Lengths for Dim-C4-CN$(PbI_3)_2$.

Atom	Atom	Length/Å
Pb(1)	I(1)1	3.2895(10)
Pb(1)	I(1)	3.1424(9)
Pb(1)	I(2)	3.1323(10)
Pb(1)	I(2)2	3.2587(10)
Pb(1)	I(3)2	3.2736(9)
Pb(1)	I(3)	3.1867(10)
N(1)	C(2)	1.462(15)
N(1)	C(3)	1.418(17)
N(1)	C(5)	1.322(14)
N(2)	C(4)	1.396(15)
N(2)	C(5)	1.336(14)
N(2)	C(6)	1.416(15)
N(3)	C(9)	1.078(18)
C(1)	C(1)3	1.41(3)
C(1)	C(2)	1.48(2)
C(3)	C(4)	1.35(2)
C(6)	C(7)	1.528(18)
C(7)	C(8)	1.545(18)
C(8)	C(9)	1.450(19)

Supplementary Table 29. Bond Angles for Dim-C4-CN(PbI_3)$_2$.

Atom	Atom	Atom	Angle/°
I(1)	Pb(1)	I(1)1	175.27(3)
I(1)	Pb(1)	I(2)2	83.68(3)
I(1)	Pb(1)	I(3)	88.88(3)
I(1)	Pb(1)	I(3)2	87.43(2)
I(2)2	Pb(1)	I(1)1	101.04(3)
I(2)	Pb(1)	I(1)	96.82(2)
I(2)	Pb(1)	I(1)1	83.34(2)
I(2)	Pb(1)	I(2)2	92.21(3)
I(2)	Pb(1)	I(3)	84.56(3)
I(2)	Pb(1)	I(3)2	171.76(2)
I(2)2	Pb(1)	I(3)2	81.20(3)
I(3)2	Pb(1)	I(1)1	93.01(2)
I(3)	Pb(1)	I(1)1	86.42(3)
I(3)	Pb(1)	I(2)2	171.50(2)
I(3)	Pb(1)	I(3)2	102.64(3)
Pb(1)	I(1)	Pb(1)2	78.12(3)
Pb(1)	I(2)	Pb(1)1	78.73(3)
Pb(1)	I(3)	Pb(1)1	77.74(2)
C(3)	N(1)	C(2)	127.4(11)
C(5)	N(1)	C(2)	126.0(12)
C(5)	N(1)	C(3)	106.6(11)
C(4)	N(2)	C(6)	125.4(10)
C(5)	N(2)	C(4)	107.1(10)
C(5)	N(2)	C(6)	127.5(10)
C(1)3	C(1)	C(2)	120(2)
N(1)	C(2)	C(1)	112.8(12)
C(4)	C(3)	N(1)	107.4(12)
C(3)	C(4)	N(2)	107.6(12)
N(1)	C(5)	N(2)	111.2(10)
N(2)	C(6)	C(7)	111.9(10)
C(6)	C(7)	C(8)	114.8(11)
C(9)	C(8)	C(7)	114.4(11)
N(3)	C(9)	C(8)	177.9(15)

Supplementary Table 30. Torsion Angles for Dim-C4-CN(PbI_3)$_2$.

A	B	C	D	Angle/°
N(1)	C(3)	C(4)	N(2)	-1.1(18)
N(2)	C(6)	C(7)	C(8)	63.4(15)
C(1)1	C(1)	C(2)	N(1)	63(3)
C(2)	N(1)	C(3)	C(4)	179.1(14)
C(2)	N(1)	C(5)	N(2)	-178.6(11)
C(3)	N(1)	C(2)	C(1)	90.4(19)
C(3)	N(1)	C(5)	N(2)	-0.6(15)
C(4)	N(2)	C(5)	N(1)	0.0(14)
C(4)	N(2)	C(6)	C(7)	81.2(15)
C(5)	N(1)	C(2)	C(1)	-92.0(18)
C(5)	N(1)	C(3)	C(4)	1.1(17)
C(5)	N(2)	C(4)	C(3)	0.8(16)
C(5)	N(2)	C(6)	C(7)	-97.3(14)
C(6)	N(2)	C(4)	C(3)	-178.0(13)
C(6)	N(2)	C(5)	N(1)	178.6(11)
C(6)	C(7)	C(8)	C(9)	-81.7(16)

Supplementary Table 31. Hydrogen Atom Coordinates (Å×104) and Isotropic Displacement Parameters (Å2×103) for Dim-C4-CN$(PbI_3)_2$.

Atom	x	y	z	U(eq)
H(1A)	5523.65	5565.1	4637.3	118
H(1B)	3968.71	5430.61	5270.9	118
H(2A)	3885.33	5642.09	2478.64	81
H(2B)	4893.06	5071.21	2169.71	81
H(3)	1069.91	5412.38	2990.59	94
H(4)	-419.82	4498.12	2502	76
H(5)	3704.13	4023.81	2178.76	53
H(6A)	281.2	3324.76	2479.88	63
H(6B)	1900.4	3159.14	2084.32	63
H(7A)	-171.41	3655.83	-292.26	73
H(7B)	255.07	2955.58	-212.1	73
H(8A)	2738.06	3308.54	-745.74	69
H(8B)	1580.46	3276.65	-2275.53	69

Supplementary Table 32. Photovoltaic parameters of 1.54 eV PSCs.

	V_{OC} (V)	J_{SC} (mA cm^{-2})	FF (%)	PCE (%)
Control	1.161	26.00	79.96	24.13
Dim-C2-CH_3	1.173	26.12	83.11	25.46
Dim-C2-CN	1.169	26.10	82.65	25.17
Dim-C4-CN	1.197	26.37	86.21	27.21

Supplementary Table 33. Photovoltaic parameters of Dim-C4-CN-modified 1.54 eV PSCs.

Scan Direction	V_{OC} (V)	J_{SC} (mA cm^{-2})	FF (%)	PCE (%)
For.	1.193	26.39	84.57	26.63
Rev.	1.197	26.37	86.21	27.21

Supplementary Table 34. Photovoltaic parameters of 1D-3D PSCs.

Year	Materials	V_{OC} (V)	J_{SC} (mA cm^{-2})	FF (%)	PCE (%) (Certified)	Refs
2020	Hydrazinium cation	1.108	24.69	78.00	21.20	[1]
2020	polymerizable propargylammonium	1.110	23.69	80.76	21.19	[2]
2020	Bipyridine	1.150	24.10	76.00	21.18	[3]
2021	Benzimidazole iodide	1.130	23.72	78.99	21.17	[4]
2021	Trimethylsulfonium	1.140	24.64	78.57	22.06	[5]
2021	Iodomethylammonium iodide	1.170	24.50	79.00	22.70	[6]
2021	2- diethylaminoethylchloride	1.220	24.00	78.00	22.90	[7]
2022	Ethane-1,2-diylbis(diphenylphosphine oxide)	1.111	24.37	79.00	21.39	[8]
2022	1-ethyl-3-methylimidazolium trifluoroacetate	1.136	23.57	82.70	22.14	[9]
2022	1,10-phenanthroline	1.120	25.4	82.00	23.3	[10]
2022	4-chlorobenzamidine hydrochloride	1.148	25.0	76.47	21.95	[11]
2022	6-aminocaproic acid iodides	1.155	25.35	78.92	23.11	[12]
2022	N,N′-dialkylbenzimidazolium iodide	1.170	25.77	80.70	24.3	[13]
2022	1-benzyl-3-methylimidazolium iodide	1.204	23.70	84.42	24.09 (23.54)	[14]
2023	1-cyanopropyl-3-methyl imidazolium chloride	1.182	25.20	81.02	24.13	[15]
2023	2-aminobenzothiazole lead iodide	1.167	23.82	83.64	23.27	[16]
2023	1,3-diisopropyl-4,5-difluorobenzimidazolium iodide	1.160	25.41	81.58	24.05	[17]
2023	(5-(1,2-dithiolan-3-yl) pentanehydrazide	1.180	25.10	81.00	23.84	[18]
2023	formamidinium-based benzamidine hydrochloride	1.189	25.37	82.50	24.90	[19]
2024	1,3-dimethylimidazolium Tetrafluoroborate	1.180	25.47	82.32	24.75	[20]
2025	thiomorpholine	1.180	25.30	85.80	25.6 (24.7)	[21]

2025	Tetrabutylammonium Thiocyanate	1.176	25.70	83.30	25.18	[22]
2025	2-TFBzAI	1.171	25.56	80.79	24.19	[23]
2025	N-methyl-1-(naphthalen-1-yl)methylammonium	1.179	25.51	84.82	25.51	[24]
This work	**Dim-C4-CN**	**1.197**	**26.37**	**86.21**	**27.21 (27.02)**	

Supplementary Table 35. Photovoltaic parameters of 2D perovskite strategy in PSCs.

Year	Materials	V_{OC} (V)	J_{SC} (mA cm^{-2})	FF (%)	PCE (%) (Certified)	Refs
2021	$(C_4H_9NH_3)_2PbI_4$	1.183	24.67	84.22	24.63 (24.35)	[25]
2021	n-Butylammonium bromide	1.210	24.57	80.00	23.78 (23.09)	[26]
2022	3-fluoro-phenethylammonium	1.150	24.90	83.46	(23.90)	[27]
2022	oleylammonium iodide	1.200	24.69	82.00	24.30	[28]
2023	fluorophenylethylammonium	1.130	24.00	78.00	21.20	[29]
2023	hexylammonium hydrobromide	1.168	25.40	81.58	24.21	[30]
2023	4-amidinopyridine	1.180	25.70	81.81	24.90	[31]
2023	amount of 2-aminoindan hydrochloride	1.165	26.22	82.20	25.12 (24.60)	[32]
2023	$(Cl4Tm)_2PbI_4$	1.125	25.96	84.32	24.60	[33]
2024	$BA_2FAPb_2I_7$	1.120	25.50	82.00	24.10	[34]
2024	2-(1-cyclohexenyl)ethyl ammonium	1.160	25.87	86.16	25.86	[35]
2024	4-hydroxybenzylamine	1.190	24.94	85.9	25.60 (25.0)	[36]
2024	n-dodecylammonium	1.203	25.07	85.00	25.61	[37]
2024	N-aminohexyl-benz[f]-phthalimide	1.170	26.10	85.40	26.10	[38]
2025	pyrenylbutanamine	1.180	25.80	83.00	25.30	[39]
2025	1-(5-phenylthiophen-3-yl) propan-2-ammounium	1.190	26.00	84.39	(26.12)	[40]
2025	nicotinamidine hydroiodide	1.182	26.24	85.50	26.52	[41]
2025	σ-bond-dominant	1.206	25.02	86.08	25.97	[42]
2025	$(DFP)PbI_4$	1.192	25.16	86.79	26.03	[43]
2025	Butylammonium iodide	1.188	25.79	82.16	25.73	[44]
2025	1,3-Propanediammonium diiodide	1.225	25.24	84.53	26.14 (25.57)	[45]
2025	Oc ligand	1.189	25.90	84.10	25.90	[46]
2025	n-hexylammonium iodide	1.218	25.10	85.12	26.02 (25.42)	[47]
2025	3-aminomethylpiperidine	1.170	25.25	85.50	25.53	[48]
2025	meta-amidinopyridine	1.195	25.53	85.50	26.05 (25.44)	[49]
This work	**Dim-C4-CN**	**1.197**	**26.37**	**86.21**	**27.21 (27.02)**	

Supplementary Table 36. Photovoltaic parameters of 1.67 eV PSCs.

	V_{OC} (V)	J_{SC} (mA cm^{-2})	FF (%)	PCE (%)
Control	1.222	21.32	81.75	21.30
Dim-C4-CN	1.253	21.55	86.82	23.45

Supplementary Table 37. Photovoltaic parameters of 1.84 eV PSCs.

	V_{OC} (V)	J_{SC} (mA cm^{-2})	FF (%)	PCE (%)
Control	1.288	16.55	83.29	17.75
Dim-C4-CN	1.324	16.85	85.17	19.00

Supplementary References

1. Yu, S. *et al.* Hydrazinium cation mixed FAPbI3-based perovskite with 1D/3D hybrid dimension structure for efficient and stable solar cells. *Chem. Eng. J.* **403**, 125724 (2021).
2. Yang, N. *et al.* An: In situ cross-linked 1D/3D perovskite heterostructure improves the stability of hybrid perovskite solar cells for over 3000 h operation. *Energy Environ. Sci.* **13**, 4344–4352 (2020).
3. Liu, P. *et al.* Lattice-Matching Structurally-Stable 1D@3D Perovskites toward Highly Efficient and Stable Solar Cells. *Adv. Energy Mater.* **10**, 1903654 (2020).
4. Zhan, Y. *et al.* Elastic Lattice and Excess Charge Carrier Manipulation in 1D–3D Perovskite Solar Cells for Exceptionally Long-Term Operational Stability. *Adv. Mater.* **33**, 2105170 (2021).
5. Ge, C. *et al.* Mixed Dimensional Perovskites Heterostructure for Highly Efficient and Stable Perovskite Solar Cells. *Sol. RRL* **6**, 2100879 (2022).
6. Zhang, H. *et al.* Highly Efficient 1D/3D Ferroelectric Perovskite Solar Cell. *Adv. Funct. Mater.* **31**, 2100205 (2021).
7. Kong, T. *et al.* Perovskitoid-Templated Formation of a 1D@3D Perovskite Structure toward Highly Efficient and Stable Perovskite Solar Cells. *Adv. Energy Mater.* **11**, 2101018 (2021).
8. Zeng, H. *et al.* Improved Performance and Stability of Perovskite Solar Modules by Regulating Interfacial Ion Diffusion with Nonionic Cross-Linked 1D Lead-Iodide. *Adv. Energy Mater.* **12**, 2102820 (2022).
9. Wei, N. *et al.* Multi-Level Passivation of MAPbI 3 Perovskite for Efficient and Stable Photovoltaics. *Adv. Funct. Mater.* **32**, 2108944 (2022).
10. Chen, Q., Deng, K., Shen, Y. & Li, L. Stable one dimensional (1D)/three dimensional (3D) perovskite solar cell with an efficiency exceeding 23%. *InfoMat* **4**, e12303 (2022).
11. Wang, J. *et al.* Growth of 1D Nanorod Perovskite for Surface Passivation in FAPbI 3 Perovskite Solar Cells. *Small* **18**, 2104100 (2022).
12. Hu, Y. *et al.* Amino Acid-Based Low-Dimensional Management for Enhanced Perovskite Solar Cells. *Sol. RRL* **6**, 2200168 (2022).
13. Chen, R. *et al.* Conformal Imidazolium 1D Perovskite Capping Layer Stabilized 3D Perovskite Films for Efficient Solar Modules. *Adv. Sci.* **9**, 2204017 (2022).
14. Zhang, Y. *et al.* Efficient Inverted Perovskite Solar Cells with a Low-Dimensional Halide/Perovskite Heterostructure. *Adv. Energy Mater.* **12**, 1–9 (2022).
15. Wang, F. *et al.* Ionic liquid engineering enabled in-plane orientated 1D perovskite nanorods for efficient mixed-dimensional perovskite photovoltaics. *InfoMat* **5**, e12459 (2023).
16. Wang, D. *et al.* Binary Microcrystal Additives Enabled Antisolvent-Free Perovskite Solar Cells with High Efficiency and Stability. *Adv. Energy Mater.* **13**, 2203649 (2023).
17. Chen, R. *et al.* Patch-healed grain boundary strategy to stabilize perovskite films for high-performance solar modules. *Nano Energy* **115**, 108759 (2023).

18. Chen, Z. *et al.* Perovskite Grain-Boundary Manipulation Using Room-Temperature Dynamic Self-Healing “Ligaments” for Developing Highly Stable Flexible Perovskite Solar Cells with 23.8% Efficiency. *Adv. Mater.* **35**, 2300513 (2023).
19. Ye, F. *et al.* Tailoring Low-Dimensional Perovskites Passivation for Efficient Two-Step-Processed $FAPbI_3$ Solar Cells and Modules. *Adv. Energy Mater.* **14**, 2302775 (2023).
20. Wang, F. *et al.* Ionic Liquid-Induced 1D Perovskite: Exploring 1D Perovskite Structure to 1D/3D Heterojunction-Based Photovoltaics. *Adv. Energy Mater.* **14**, 2400021 (2024).
21. Li, S. *et al.* Anion-Cation Synergistic Regulation of Low-Dimensional Perovskite Passivation Layer for Perovskite Solar Cells. *Adv. Mater.* **37**, 2500988 (2025).
22. Wang, F. *et al.* Ionic liquid engineering enables 1D/3D perovskite photovoltaics with > 25 % efficiency: A real-time study exploring formation mechanism of 1D perovskites. *Nano Energy* **129**, 110063 (2024).
23. Yun, Y. *et al.* Dimensional engineering of interlayer for efficient area perovskite solar cells with high stability under ISOS-3 aging test. *Sci. Adv.* **3112**, 1–11 (2025).
24. Liang, L. *et al.* Formation Dynamics of Thermally Stable 1D/3D Perovskite Interfaces for High-Performance Photovoltaics. *Adv. Mater.* **37**, 2413841 (2025).
25. Jang, Y.-W. *et al.* Intact 2D/3D halide junction perovskite solar cells via solid-phase in-plane growth. *Nat. Energy* **6**, 63–71 (2021).
26. Yang, G. *et al.* Stable and low-photovoltage-loss perovskite solar cells by multifunctional passivation. *Nat. Photonics* **15**, 681–689 (2021).
27. Chen, H. *et al.* Quantum-size-tuned heterostructures enable efficient and stable inverted perovskite solar cells. *Nat. Photonics* **16**, 352–358 (2022).
28. Azmi, R. *et al.* Damp heat – stable perovskite solar cells with tailored-dimensionality 2D / 3D heterojunctions - Supplementary Materials. *Science.* **376**, 73–77 (2022).
29. Luo, L. *et al.* Stabilization of 3D/2D perovskite heterostructures via inhibition of ion diffusion by cross-linked polymers for solar cells with improved performance. *Nat. Energy* **8**, 294–303 (2023).
30. Luo, Y. *et al.* Dissolved-Cl2 triggered redox reaction enables high-performance perovskite solar cells. *Nat. Commun.* **14**, 3738 (2023).
31. Yang, T. *et al.* Amidino-based Dion-Jacobson 2D perovskite for efficient and stable 2D/3D heterostructure perovskite solar cells. *Joule* **7**, 574–586 (2023).
32. Li, H. *et al.* 2D/3D heterojunction engineering at the buried interface towards high-performance inverted methylammonium-free perovskite solar cells. *Nat. Energy* **8**, 946–955 (2023).
33. Ma, K. *et al.* Holistic energy landscape management in 2D/3D heterojunction via molecular engineering for efficient perovskite solar cells. *Sci. Adv.* **9**, 1–10 (2023).
34. Sidhik, S. *et al.* Two-dimensional perovskite templates for durable, efficient

formamidinium perovskite solar cells. *Science.* **384**, 1227–1235 (2024).
35. Wang, H. *et al.* Impurity-healing interface engineering for efficient perovskite submodules. *Nature* **634**, 1091–1095 (2024).
36. Azmi, R. *et al.* Double-side 2D/3D heterojunctions for inverted perovskite solar cells. *Nature* **628**, 93–98 (2024).
37. Li, J. *et al.* Homogeneous coverage of the low-dimensional perovskite passivation layer for formamidinium–caesium perovskite solar modules. *Nat. Energy* **9**, 1540–1550 (2024).
38. Liu, C. *et al.* Two-dimensional perovskitoids enhance stability in perovskite solar cells. *Nature* **633**, 359–364 (2024).
39. Zhang, J. *et al.* Engineering Spacer Conjugation for Efficient and Stable 2D/3D Perovskite Solar Cells and Modules. *Angew. Chemie Int. Ed.* **64**, e202413303 (2025).
40. Yan, G., Tang, H., Shen, Y., Han, L. & Han, Q. AI-Generated Ammonium Ligands for High-Efficiency and Stable 2D/3D Heterojunction Perovskite Solar Cells. *Adv. Mater.* **37**, 2503154 (2025).
41. Zhang, X. *et al.* Amidinium-Based 2D Spacer Cations Enhance Efficiency and High-Temperature Photostability of Perovskite Solar Cells. *Adv. Mater.* **37**, 2504351 (2025).
42. Li, Z. *et al.* Synthesis of a lattice-resolved laminate-structured perovskite heterointerface. *Nat. Synth.* **4**, 1078–1087 (2025).
43. Song, Z. *et al.* Buried and bulk synergistic engineering enables high-performance inverted 2D/3D perovskite solar cells. *Energy Environ. Sci.* **18**, 3740–3749 (2025).
44. Chen, J. *et al.* Surface Template Realizing Oriented Perovskites for Highly Efficient Solar Cells. *Adv. Mater.* **37***,* 2417054 (2025).
45. Xu, Y. *et al.* Multicomponent Solvent Engineered Spatially Uniform 2D/3D Perovskite Heterojunction for Solar Cells. *ACS Energy Lett.* **10**, 2035–2044 (2025).
46. Tan, S. *et al.* Spontaneous formation of robust two-dimensional perovskite phases. *Science.* **388**, 639–645 (2025).
47. Zhang, Z. *et al.* Anti-solvent engineering for efficient and stable perovskite solar cells with preferentially orientated 2-dimensional/3-dimensional heterojunctions. *Energy Environ. Sci.* **18**, 3223–3234 (2025).
48. Ramakrishnan, S. *et al.* Phase-stabilized 2D/3D hetero-bilayers via lattice matching for efficient and stable inverted solar cells. *Joule* **9**, 101954 (2025).
49. Chang, X. *et al.* Solvent-dripping modulated 3D/2D heterostructures for high-performance perovskite solar cells. *Nat. Commun.* **16**, 1042 (2025).